Observing Interannual Variations in Hadley Circulation Atmospheric Diabatic Heating and Circulation Strength

Norman G. Loeb[1], David Rutan[2], Seiji Kato[1], Weijie Wang[2,3]

[1]NASA Langley Research Center, Hampton, VA
[2]Science Systems and Applications, Inc., Hampton, VA
[3]Scripps Institute of Oceanography, La Jolla, CA

March 17, 2014, AIRS Science Team Meeting, Pasadena, CA

Outline

- Earth's Energy Budget
- Using an Energetic Perspective to Observe Variations in Large-Scale Circulation
- Co-variability of cloud radiative effects and circulation

Earth's Energy Budget (1σ Range)

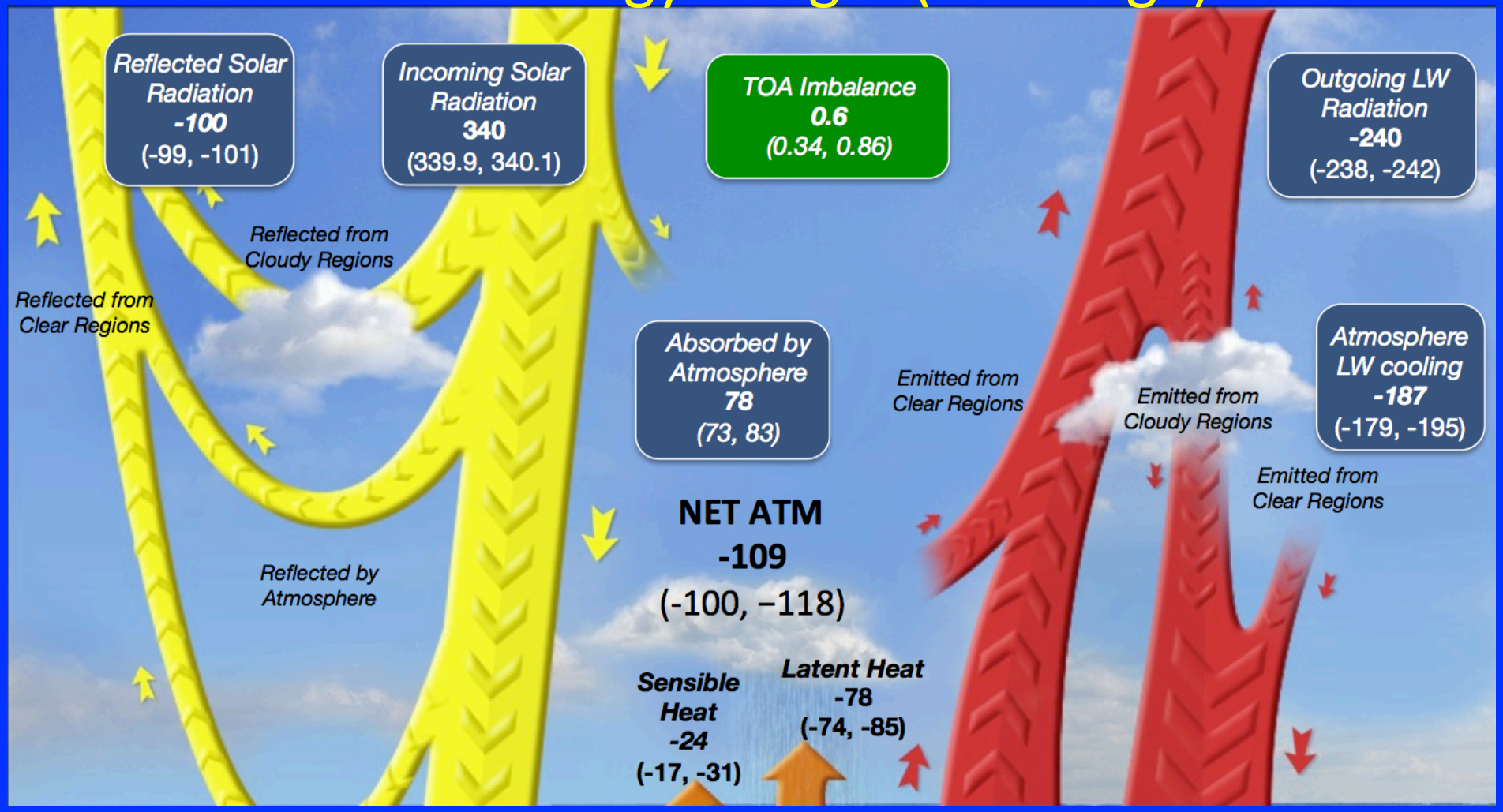

The radiative imbalance between the surface and atmosphere determines how much energy is available to drive the hydrological cycle and the exchange of sensible heat between the surface and atmosphere.

Why It's Important to Understand Earth's Radiation Budget

CERES Net TOA Radiation
(EBAF Ed2.6r Climatology: March 2000-June 2011)

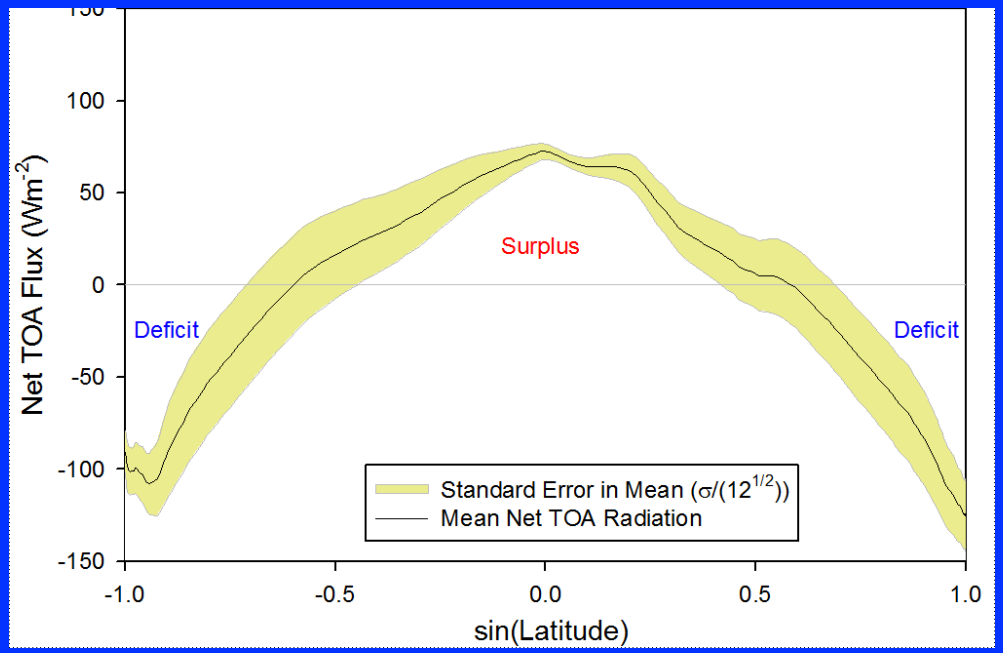

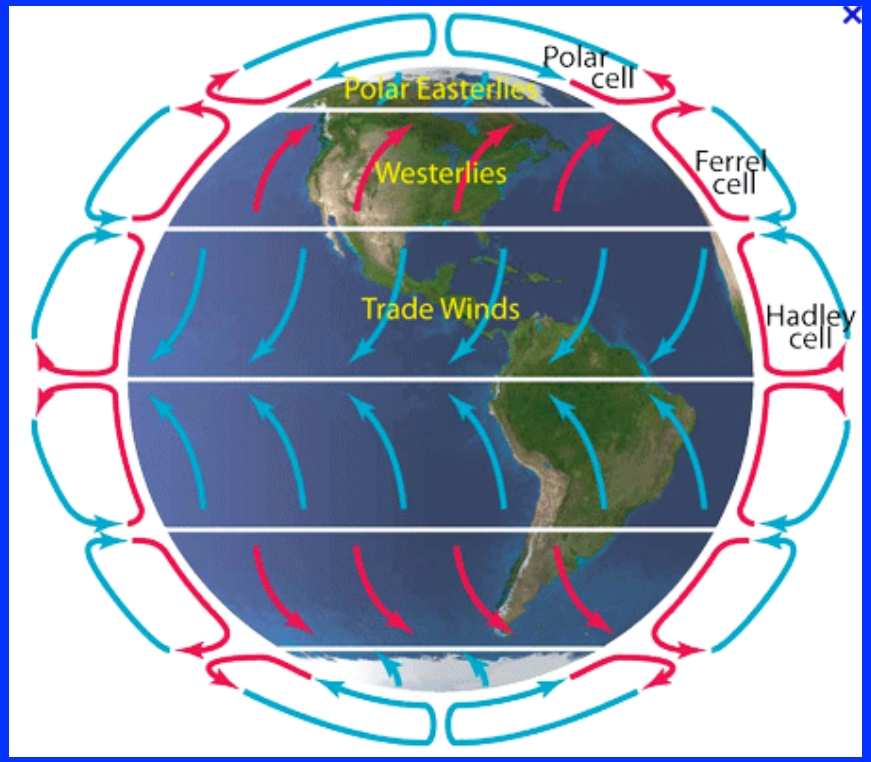

- Radiation imbalance between low and high latitudes is balanced by equator-to-pole heat transported by the atmosphere and oceans.
- The regional pattern of net radiation drives the atmospheric and oceanic circulations.

CERES Data Fusion: Net Radiative Effects of Clouds on Earth's Radiation Budget

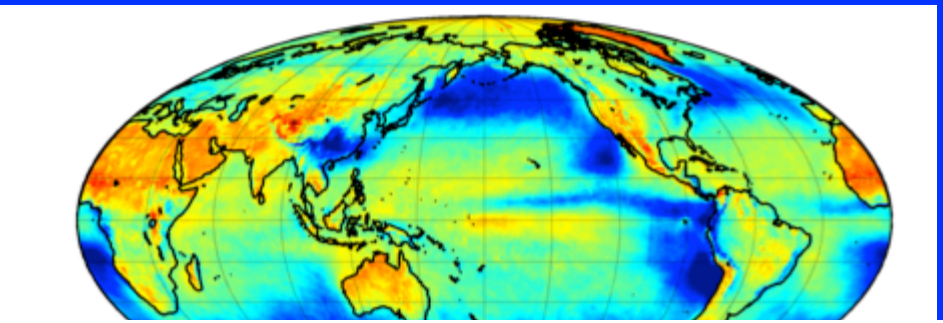

Top-of-Atmosphere (-20.9 Wm^{-2})

- SORCE-TIM: Solar Irradiance
- CERES: Reflected Solar, Emitted Thermal Flux
- MODIS: Cloud Detection & Properties
- 5 Geo Satellites: Diurnal Cycle

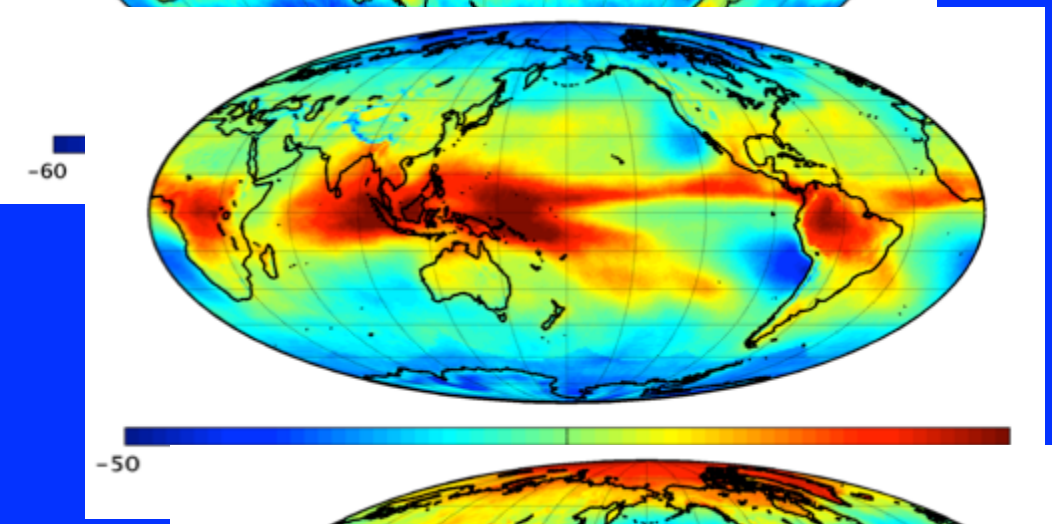

Within-Atmosphere (0.4 Wm^{-2})

- MODIS: Aerosol & Cloud Properties
- GMAO Reanalysis: Atmospheric State
- Aerosol Assimilation
- Constraints from: AIRS, CALIPSO, CloudSat

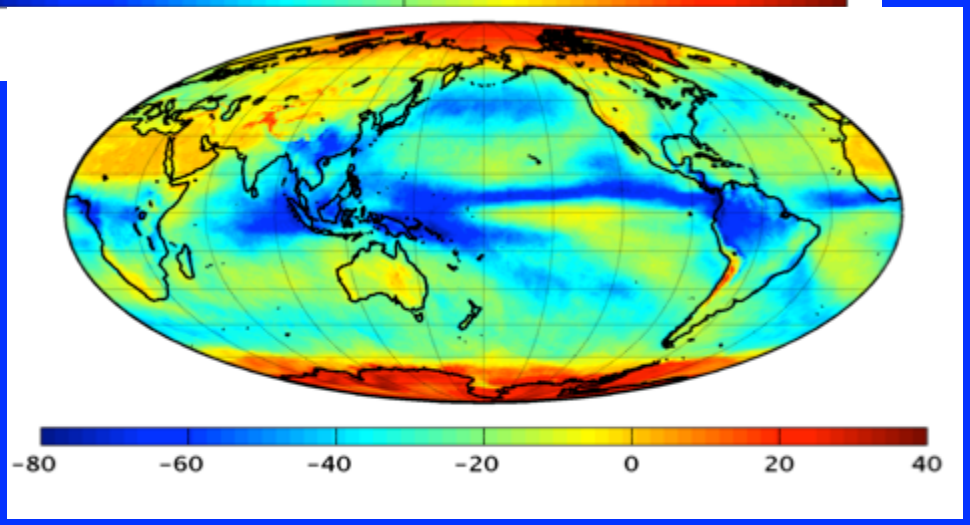

Surface (-21.3 Wm^{-2})

- MODIS: Surface albedo, emissivity & temperature
- NSIDC: Snow, sea-ice coverage

Global TOA All-Sky Radiation Anomalies
(CERES_EBAF_Ed2.8; 03/2000 – 10/2013)

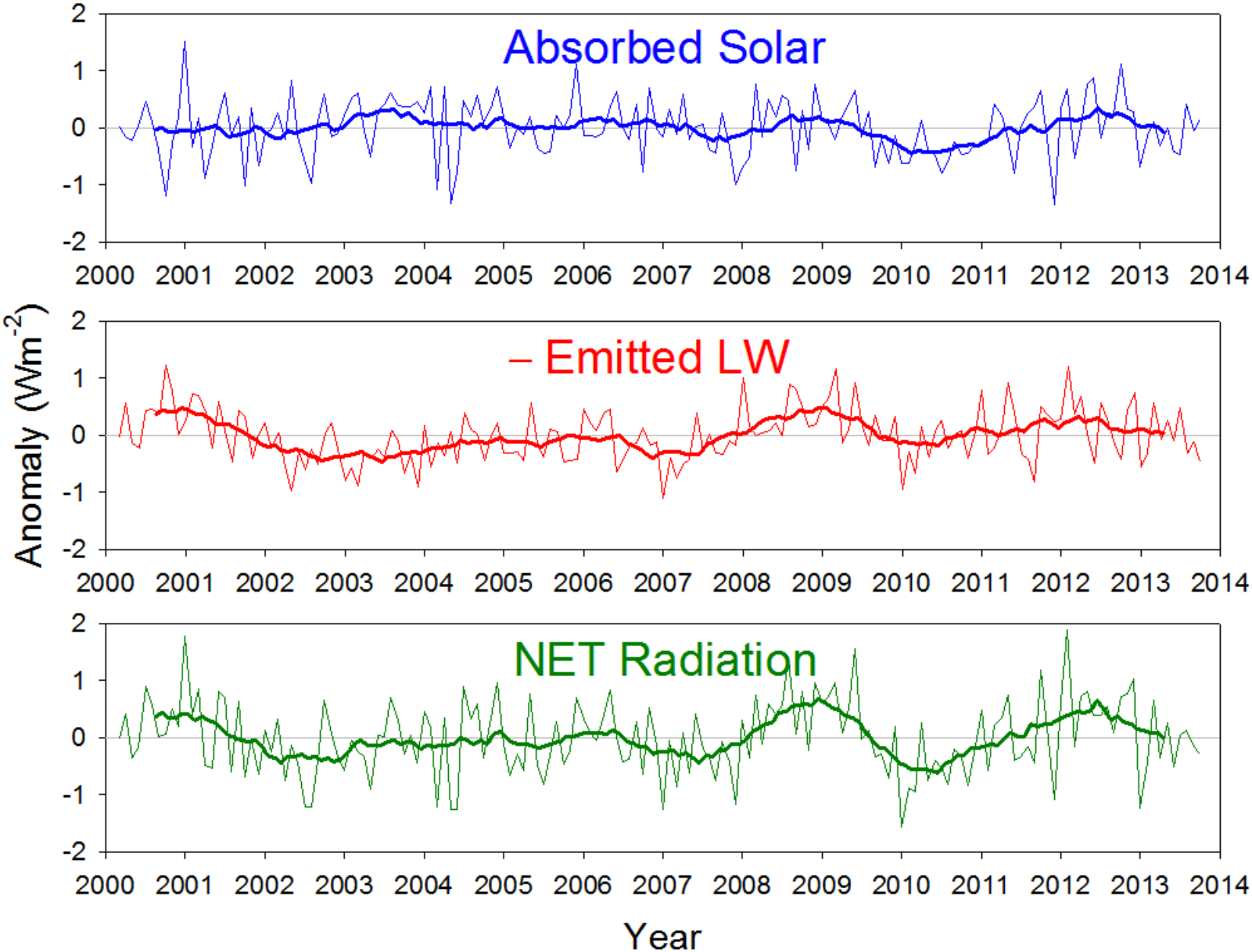

TOA Radiation Changes (March 2000 – October 2013)

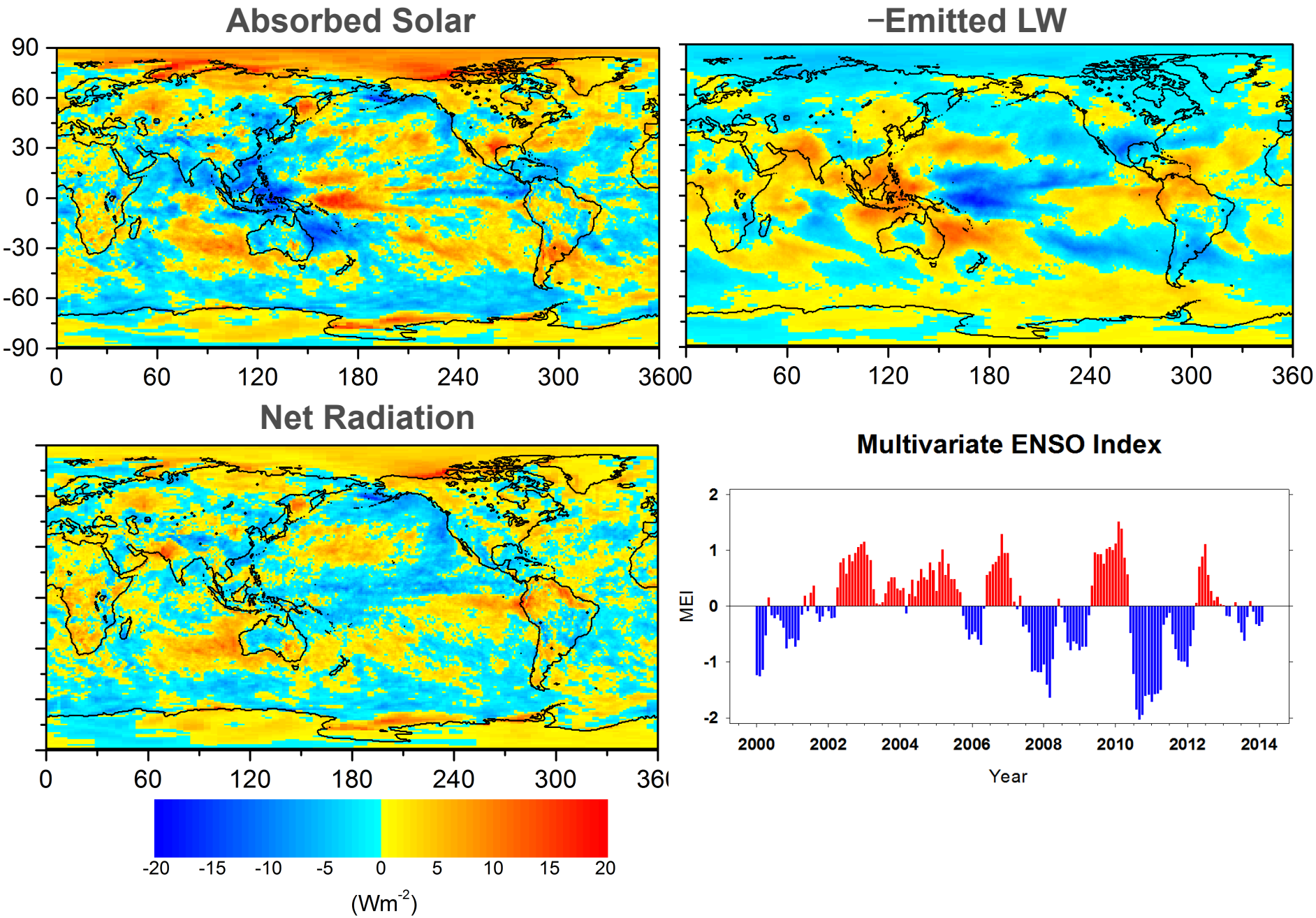

Using an Energetic Perspective to Observe Variations in Large-Scale Circulation

- Explore use of satellite observations and reanalysis to observe interannual variations in Hadley Circulation strength implied by atmospheric diabatic heating within the branches of the Hadley Circulation.
- Stratify data according to large-scale domains corresponding to ascending and descending branches of Hadley Circulation.
- How do interannual variations in atmospheric radiation, precipitation, sensible heat and dry static energy divergence co-vary in different circulation regimes?
- How do clouds influence the atmospheric energy budget in the different branches of the Hadley Circulation.

Dry Static Energy Budget

- On annual mean time-scale:

$$R_a + LP + S = H$$

R_a = net atmospheric radiation (=$R_{toa} - R_{sfc}$)
P = precipitation rate
L = Latent heat of vaporization
S = Surface sensible heat flux
H = Vertical integral of divergence of dry static and kinetic energy.

$$H = \boldsymbol{\nabla}.\frac{1}{g}\int_0^{p_s}(s+k)\boldsymbol{v}dp$$

where $s=c_p T + gz$ is the dry static energy and k is kinetic energy.

Data Used

1) Reanalysis

- ERA-Interim monthly meridional wind profiles, surface sensible heat flux, 500 hPa vertical velocity, vertical integral of dry static energy divergence.
- MERRA V5.2: 500 hPa vertical velocity, vertical integral of dry static energy divergence.

2) Satellite

- CERES EBAF Ed2.7 TOA and SFC radiation (March 2000-September 2012).
- GPCP V2.2, TRMM 3A12, TRMM 3B31 precipitation.

Mass Weighted Zonal Mean Meridional Stream Function (October 2011)

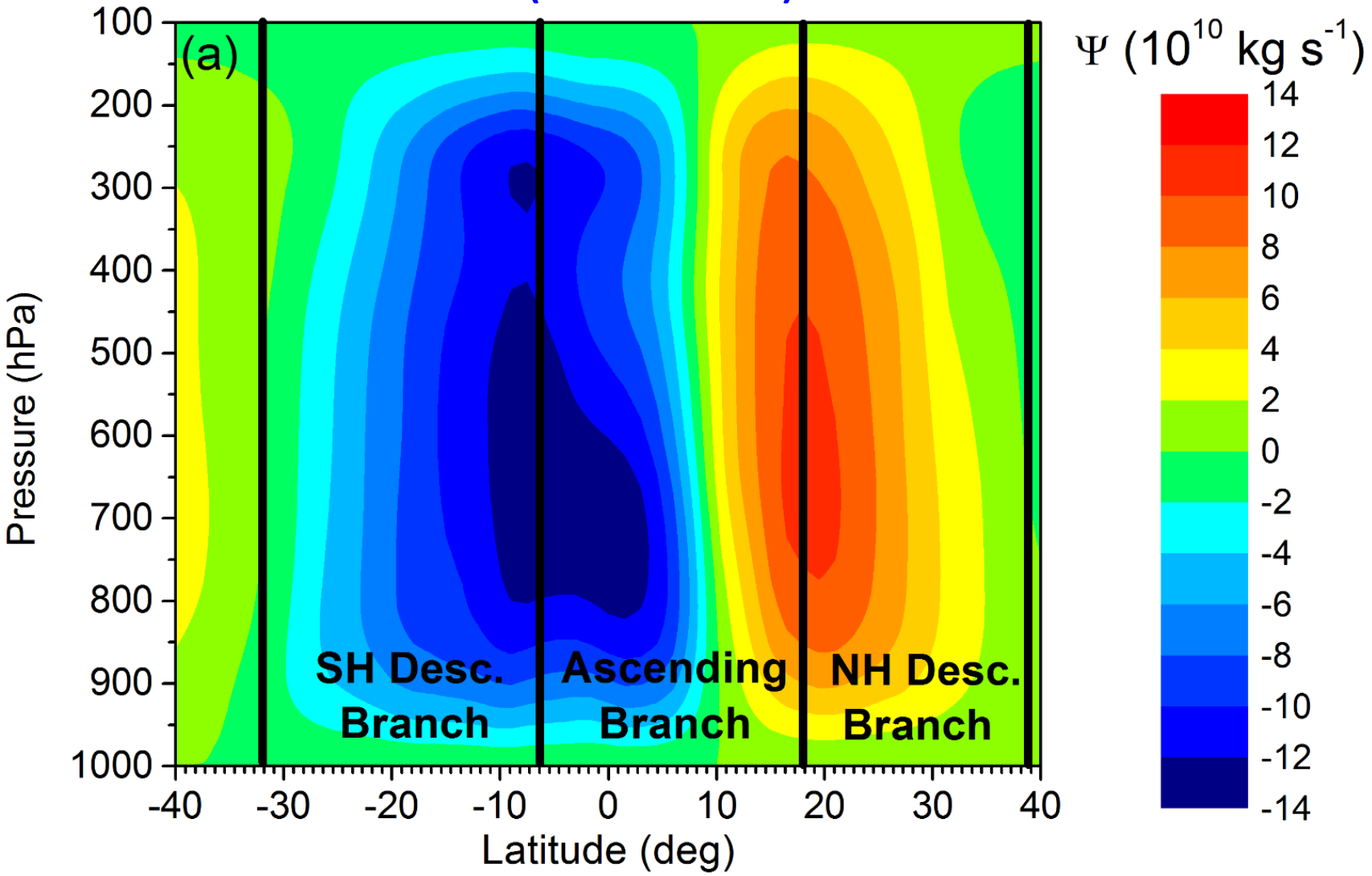

Mean (March 2000-February 2010) TOA LW CRE and SW CRE

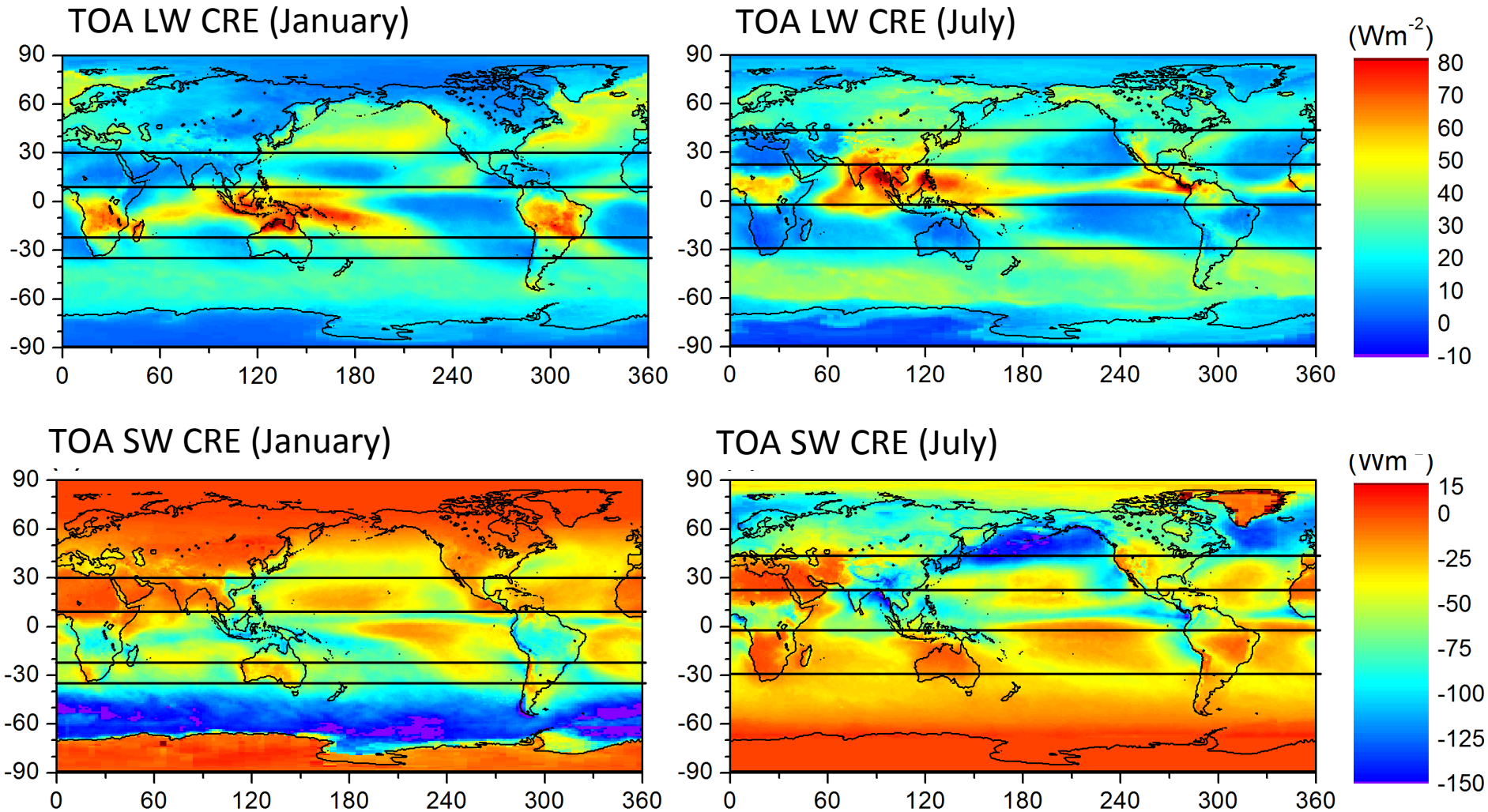

Solid lines show boundaries of ascending and descending branches of the Hadley circulation.

Mean Cloud Fraction (MODIS)

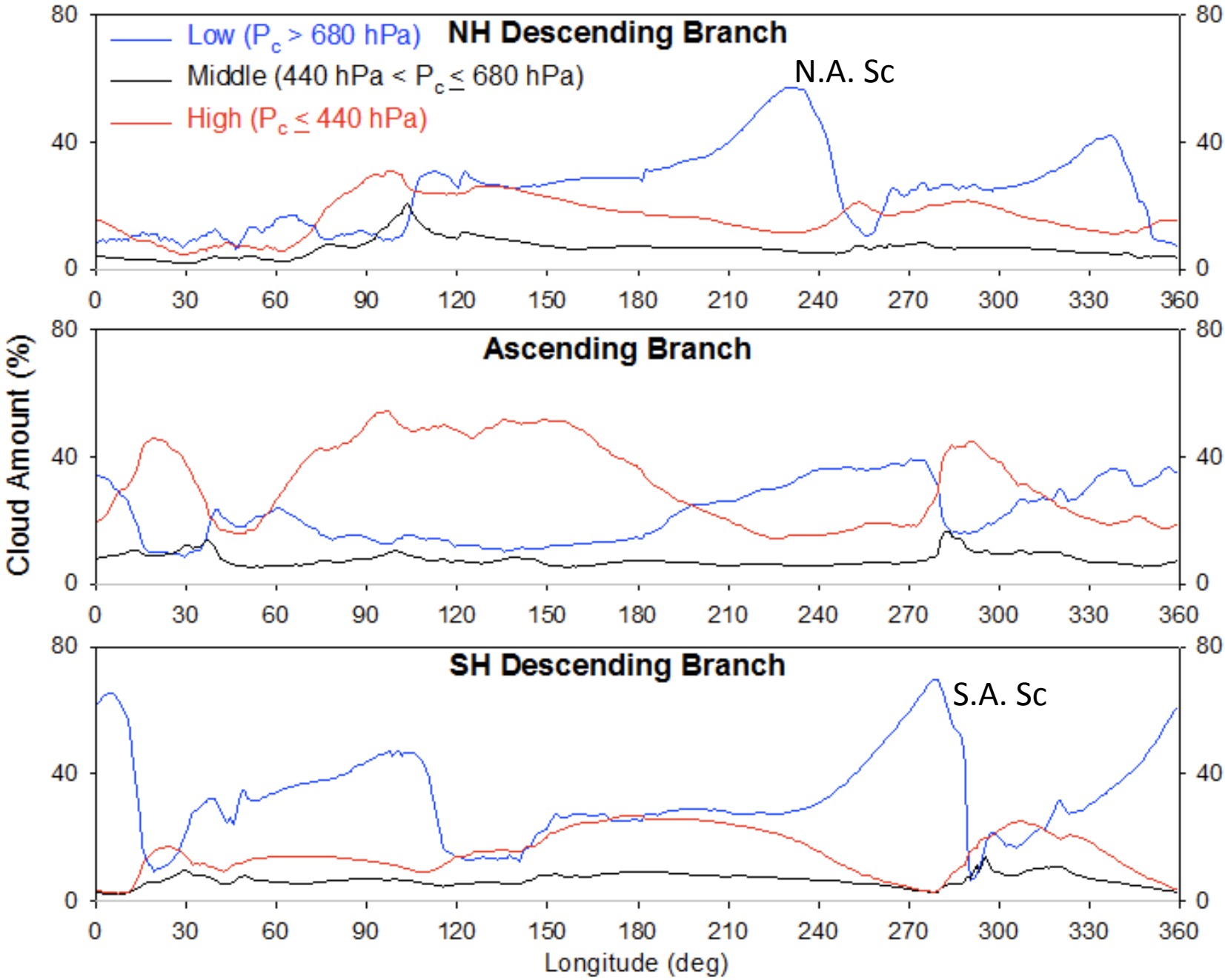

Evaluation of Hadley Circulation Boundaries

Zonal Mean CERES LW CRE for January

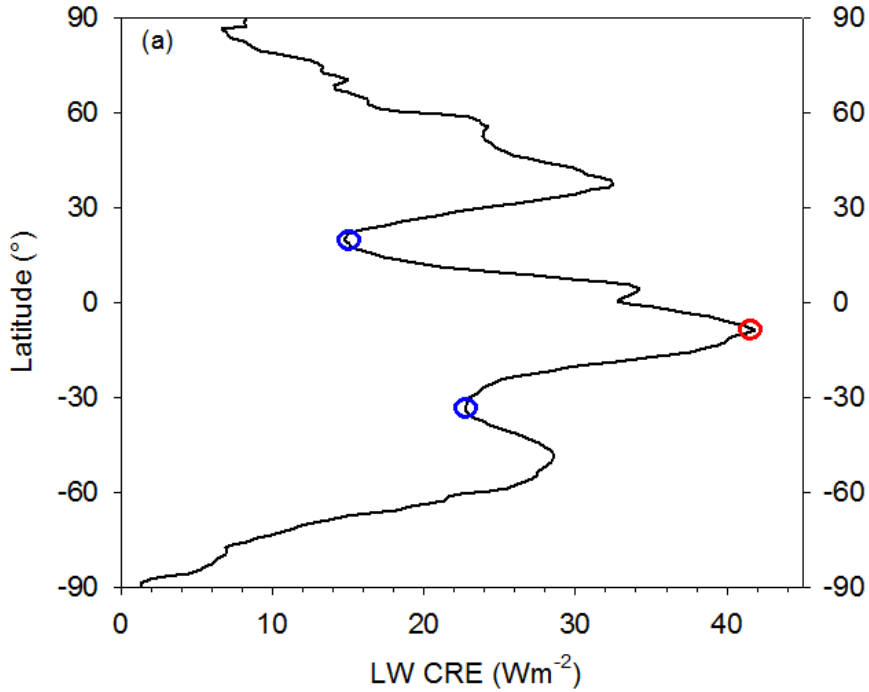

Annual Cycle of HC Boundaries & LW CRE Extrema

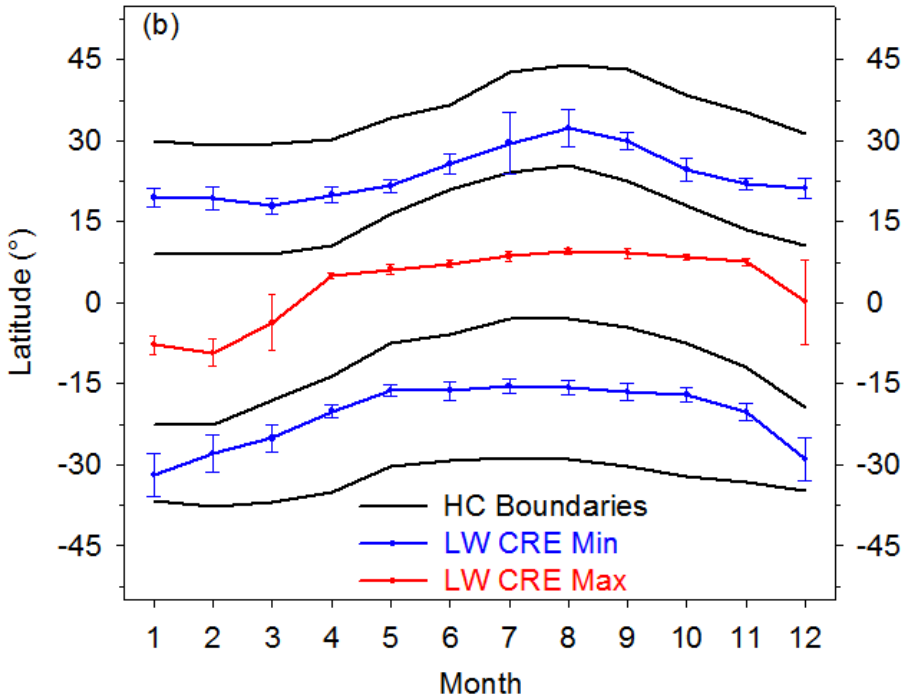

- Minima in LW CRE correspond to the latitude where subsidence reaches a maximum.
- Maximum LW CRE corresponds to the latitude of maximum convection (ITCZ).
- Both track positions of HC boundaries.
- The variability in descending branches is smallest in the wintertime when the HC is strongest (evident from the error bars).

Twelve-month Running Average of Latitudinal Distance Between Positions of NH and SH Subtropical Minima in LW CRE

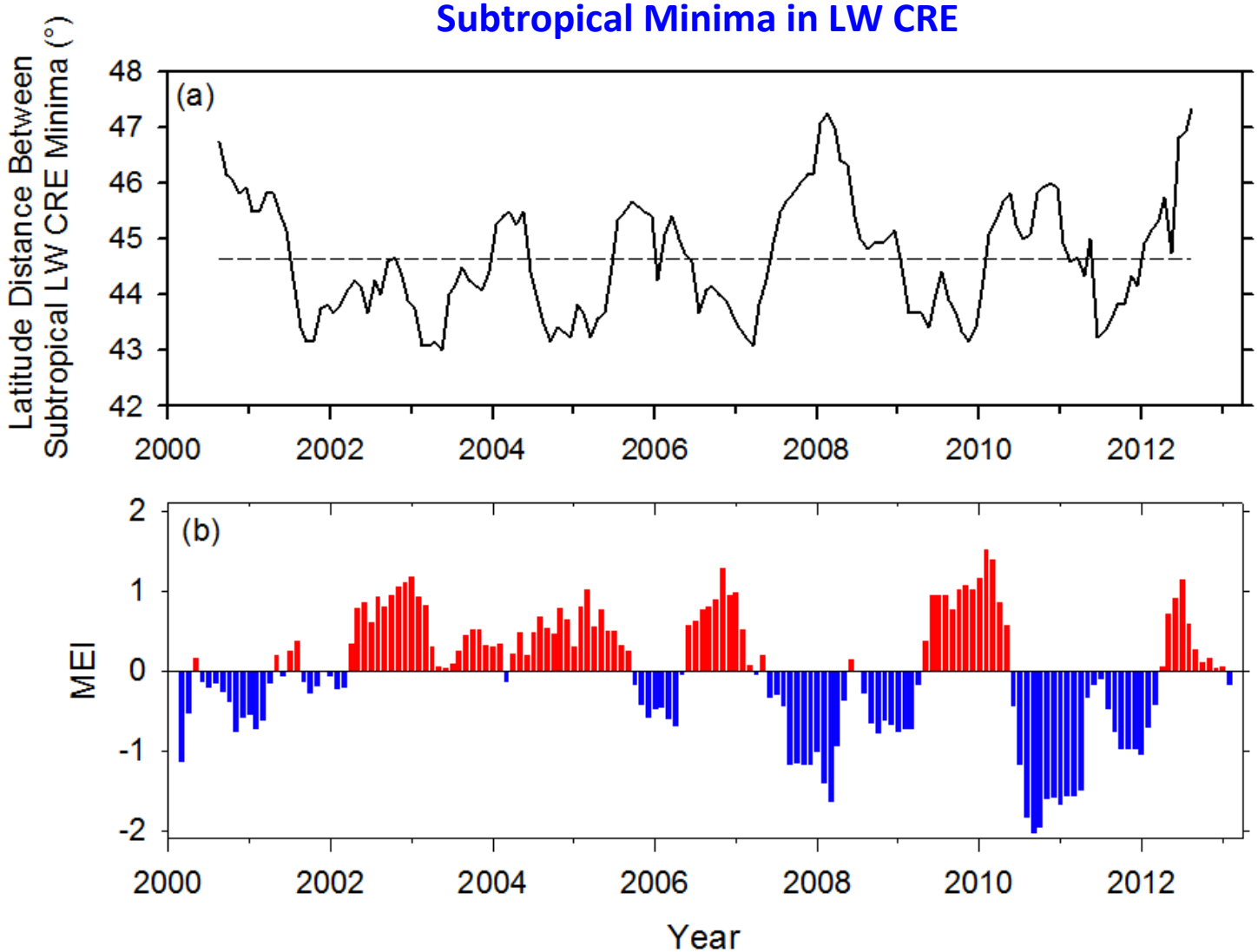

- Width between the positions of NH & SH subtropical maximum subsidence is greater during La Niña (expansion of HC) and smaller (contraction of HC) during El Niño conditions.

Mean of Atmospheric Energy Budget Terms By Longitude (Mar 2000-Feb 2010)

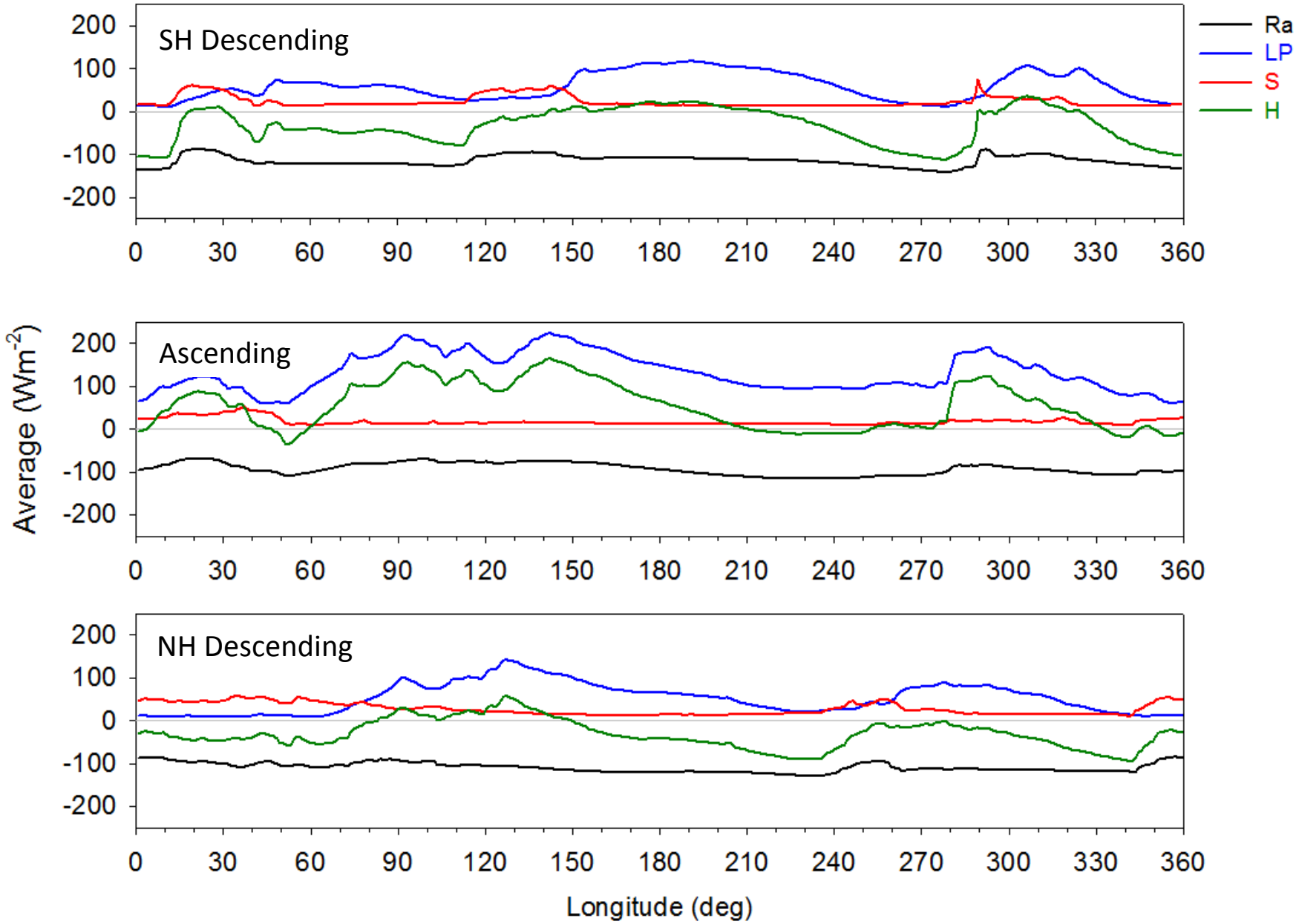

Twelve-month running average of the heat budget terms

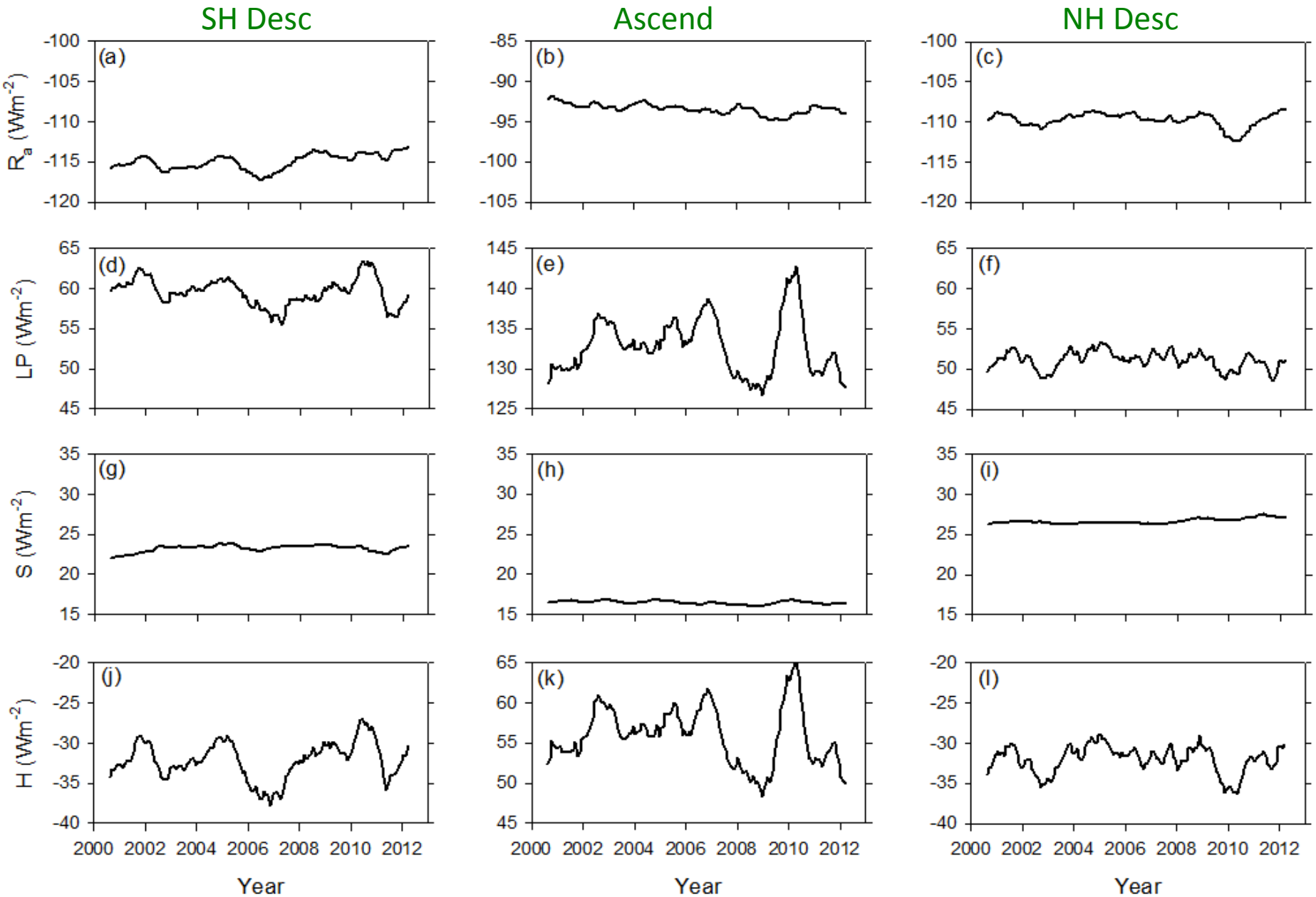

Twelve-month running average of global mean Ra+S and LP, H

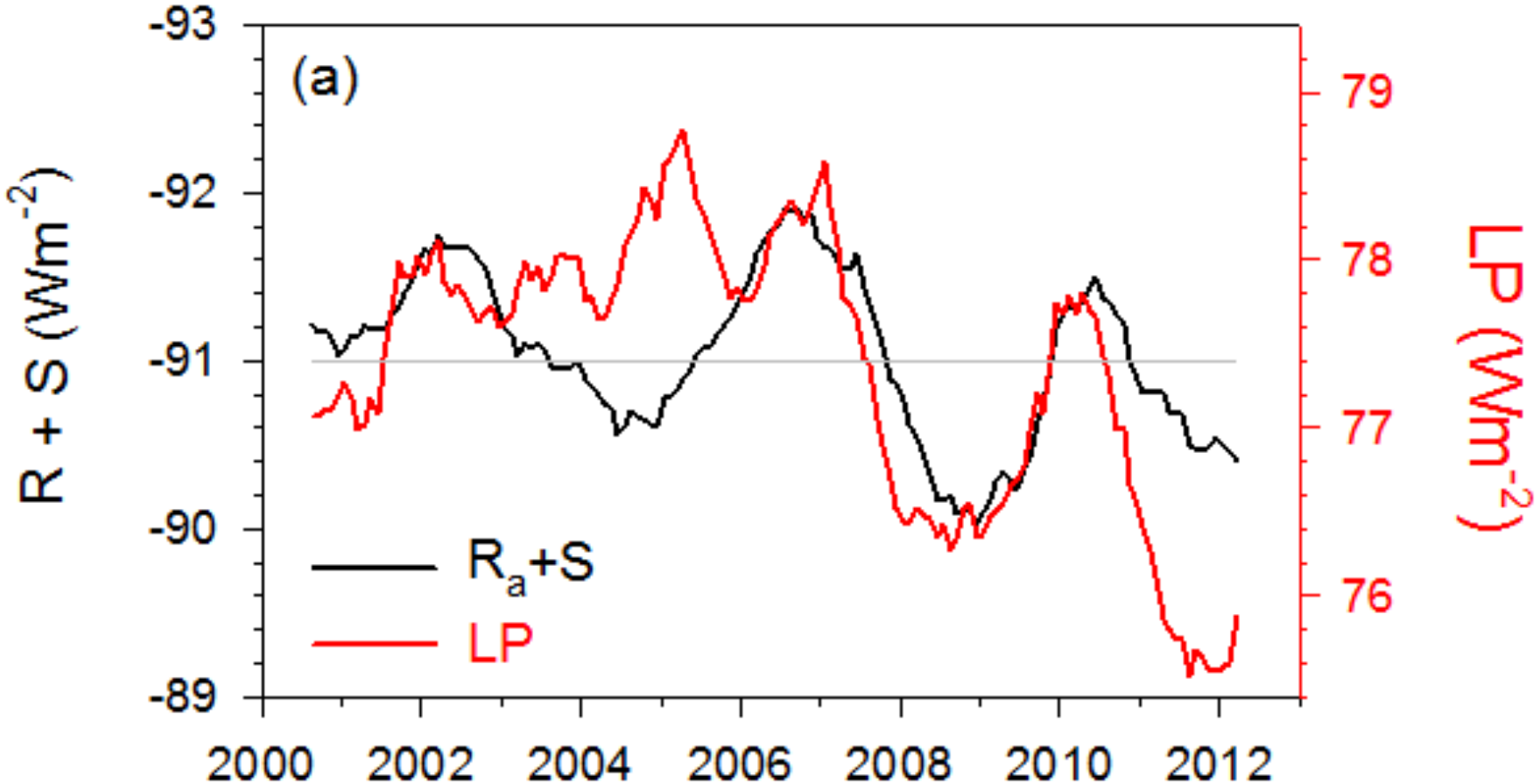

- Despite -14 Wm^{-2} imbalance in global atmospheric energy balance, interannual variations in LP and Ra are consistent.
- Largest discrepancies occur at extrema in LP (2005 and 2012).
- During stronger ENSO conditions, Ra+S and LP track one another closely.

GPCP minus TRMM (3A12) LP difference (March 2000-September 2012)

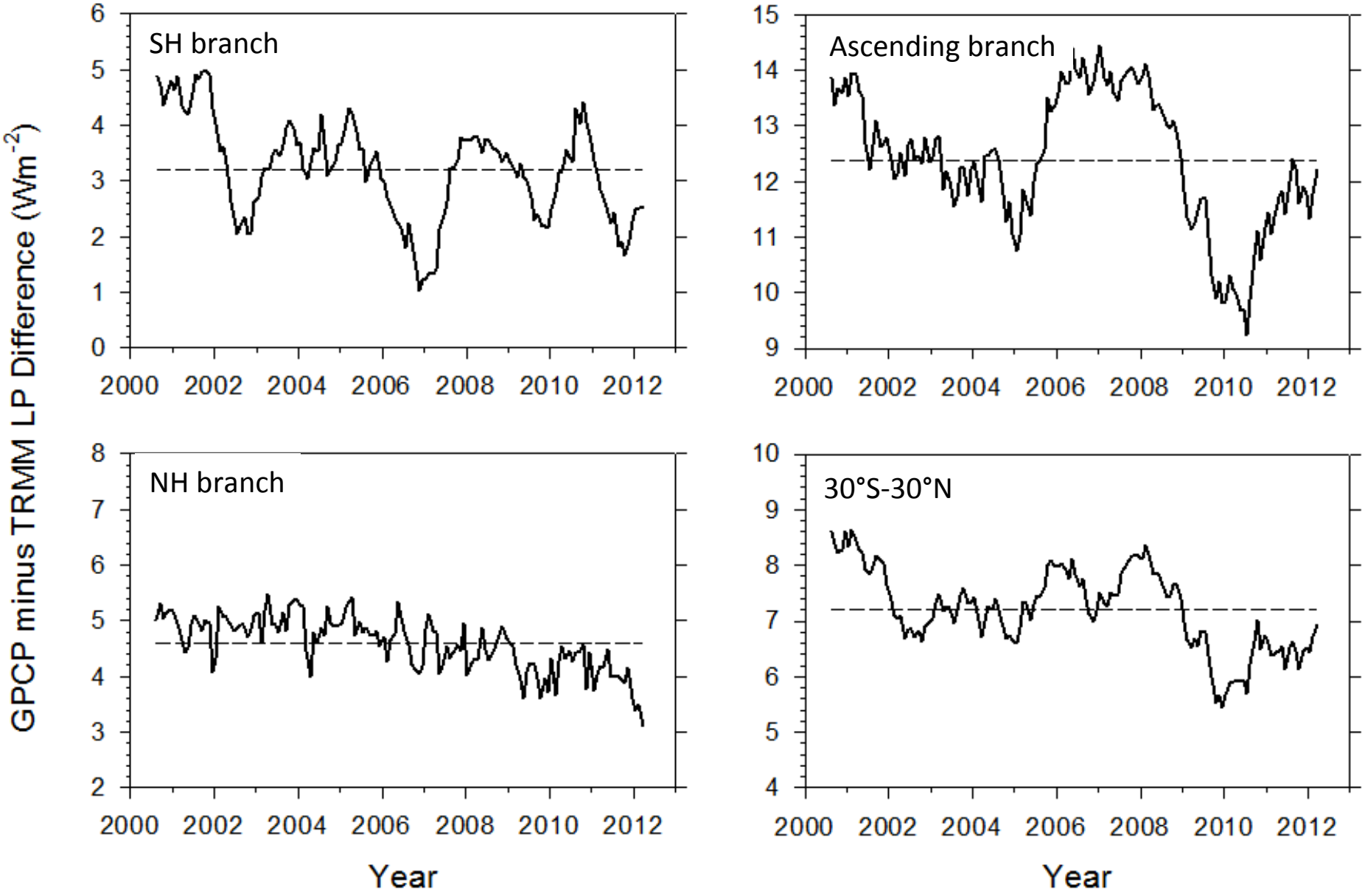

Average (Stdev) in LP for GPCP V2.2, TRMM (3A12), TRMM (3B43) (March 2000-Sept 2012)

	SH	Asc	NH	30ºS-30ºN
GPCP V2.2	59.6 (1.7)	132.8 (3.5)	51.1 (1.1)	88.4 (0.92)
TRMM_3A12	56.4 (1.2)	120.4 (0.73)	46.5 (0.73)	81.2 (0.73)
TRMM_3B43	57.1 (2.2)	142.4 (2.3)	52.5 (1.7)	93.3 (1.3)

The three data products agree to:

- 3 Wm^{-2} (5%) in the SH descending branch
- 6 Wm^{-2} (12%) in the NH descending branch
- **22 Wm^{-2} (17%) in the ascending branch**
- 12 Wm^{-2} (14%) for 30°S-30°N

Colocated PR and CloudSat Rain Rate Distributions

- Justification in Stephens et al (2012) for increasing Latent Heat Flux is based upon comparisons between CloudSat and TRMM PR in tropics.

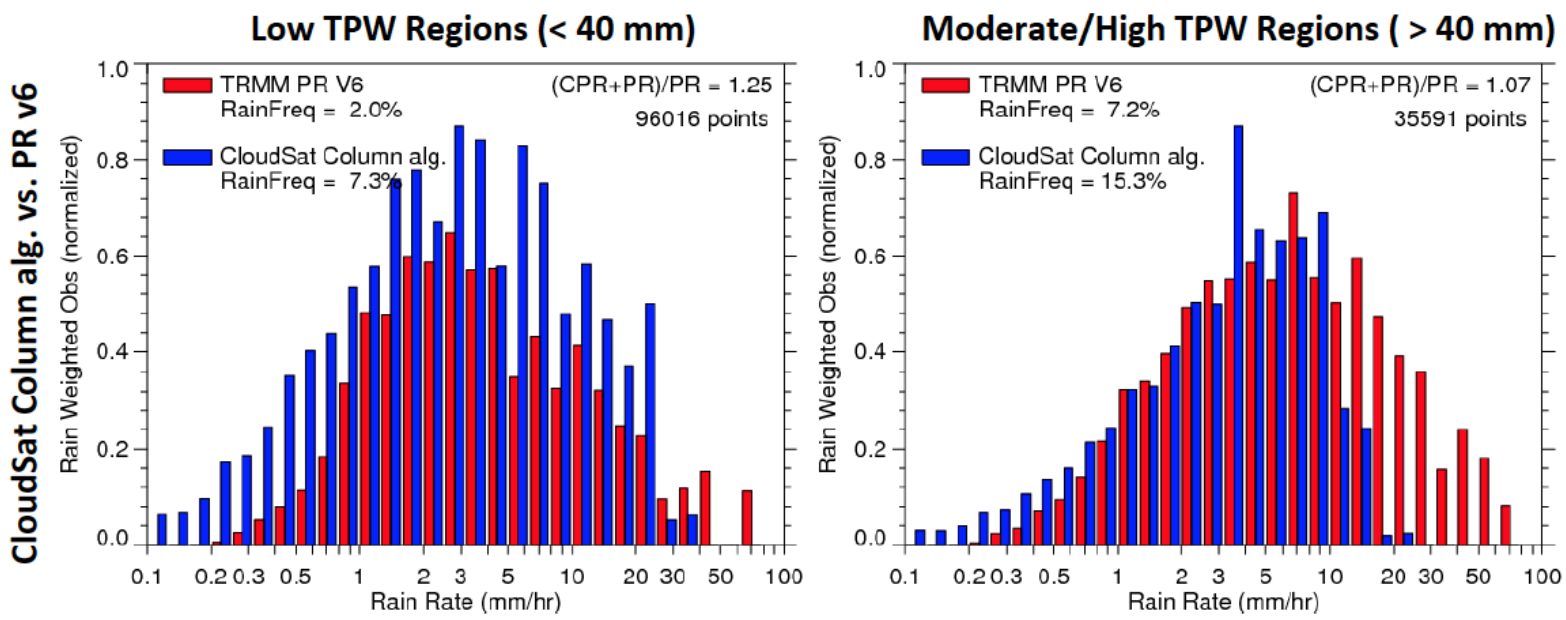

Rain Volume
- PR misses ~10%

Rain Fraction
- PR -> 3.7%
- CPR -> 8.9%

- TRMM PR misses approximately **10%** of total rain.

Berg et al. (2010)

Collocated PR and CloudSat Rain Rate Distributions (Updated Analysis)

- CloudSat data reprocessed with Lebsock
- TRMM PR V7 released.

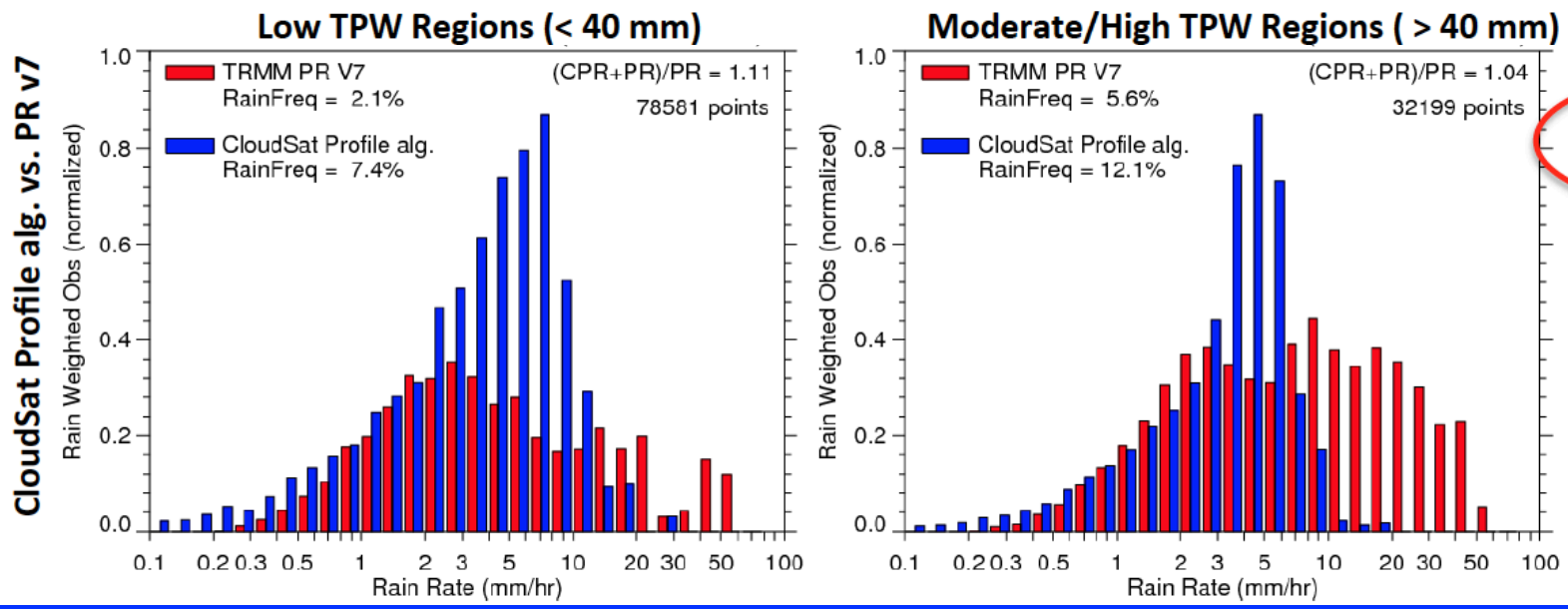

Rain Volume
- PR misses ~5%

Rain Fraction
- PR -> 3.7%
- CPR -> 8.8%

Good agreement in 1-2 mm/hr range.

- TRMM PR now misses approximately **5%** of total rain.
- GPCP is consistent with TRMM PR V7 in tropics.
- Larger uncertainty at mid-to-high latitudes (GPM will help quantify uncertainty).

Berg (personal communication)

AIRS and CERES Global Mean OLR Anomaly Time Series (W/m^2)
September 2002 through August 2013

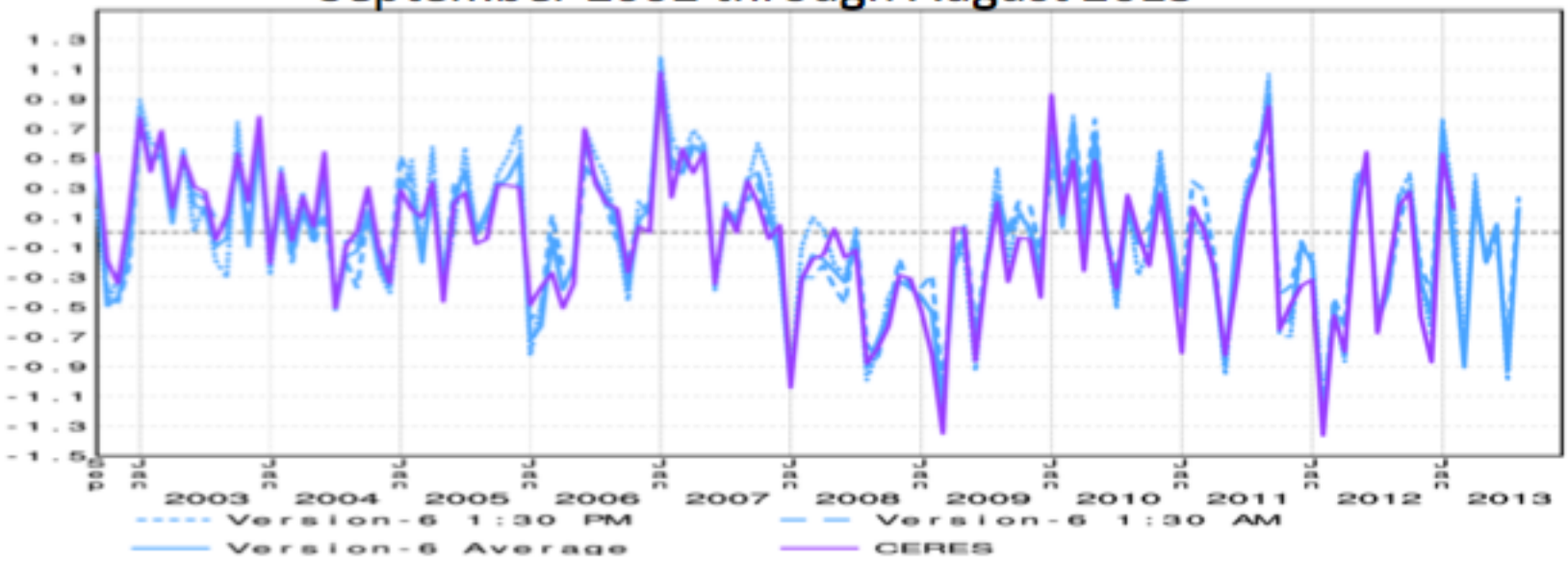

Difference in AIRS minus CERES trend < 0.2 Wm^{-2} per decade

Susskind's ~~Oct 15, 2013~~ Cancelled AIRS STM presentation

Validation of CERES EBAF-Surface Radiation

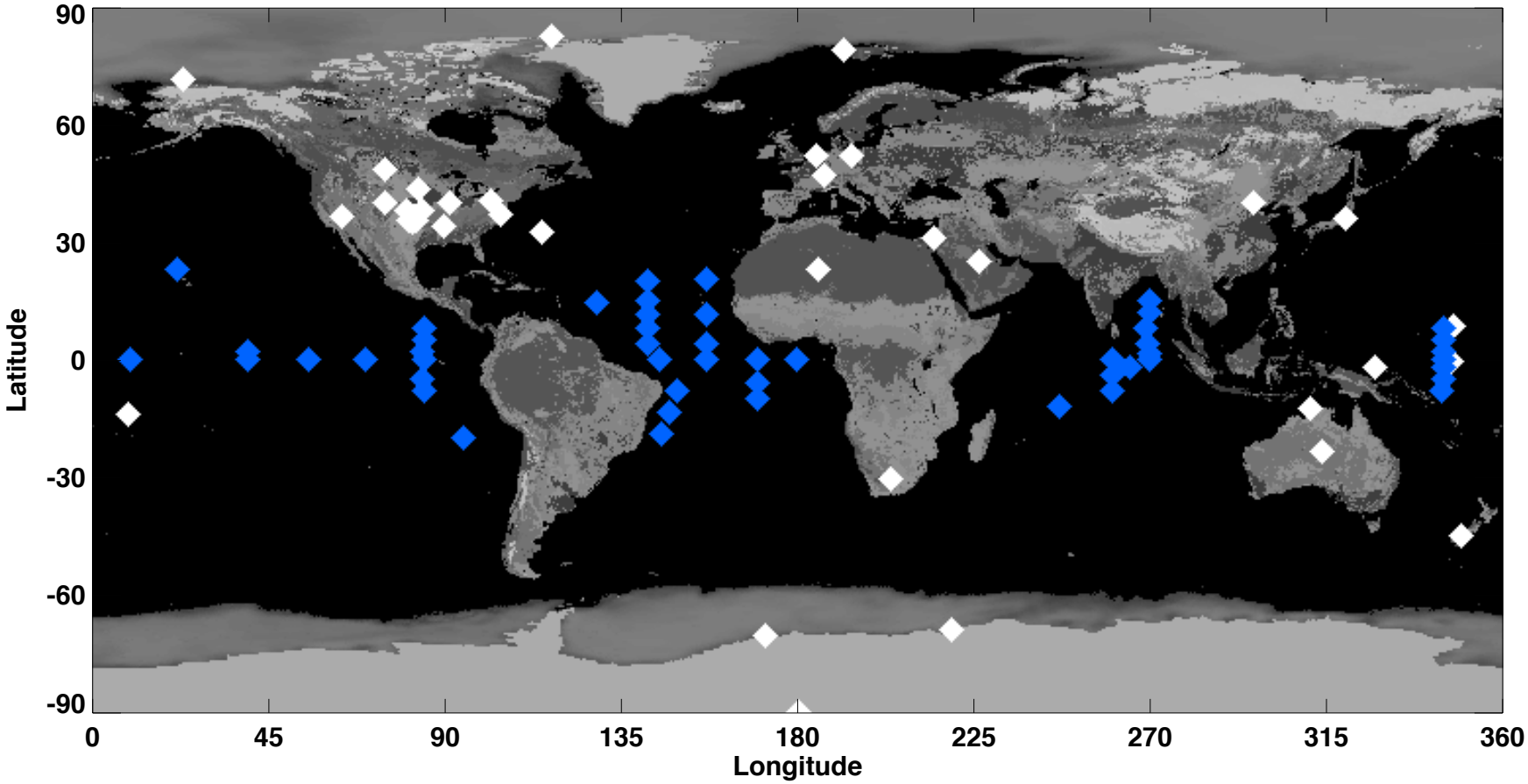

49 Ocean Buoy Sites

37 Land Sites

Surface Observed Irradiance Data Providers*			
Land & Island Locations		*Number Of Sites; Web Site*	
Baseline Surface Radiation Network (BSRN)	Many generous institutions!	20	www.bsrn.awi.de
US Dept. of Energy	Atmospheric Radiation Measurement Program (ARM)	9	www.arm.gov
NOAA - Global Monitoring Division (GMD)	Surface Radiation Network (SURFRAD)	8	www.esrl.noaa.gov/gmd/grad/field.html
Ocean Buoys			
NOAA - Pacific Marine Environmental Labs (PMEL)	Buoy Data: PIRATA, RAMA & TAO buoy arrays	46	www.pmel.noaa.gov/tao/index.shtml
Woods Hole Oceanographic Institute (WHOI)	Upper Ocean Processes Group: NTAS, WHOTS, & Stratus Long Term Buoys	3	uop.whoi.edu/projects/projects.htm
**All sites do not have continuous data records over the 12 year EBAF time period.*			

Monthly Anomalies in Downward Surface Flux from CERES EBAF & Surface Observations (Approx. 30 Land and 19 Ocean sites)

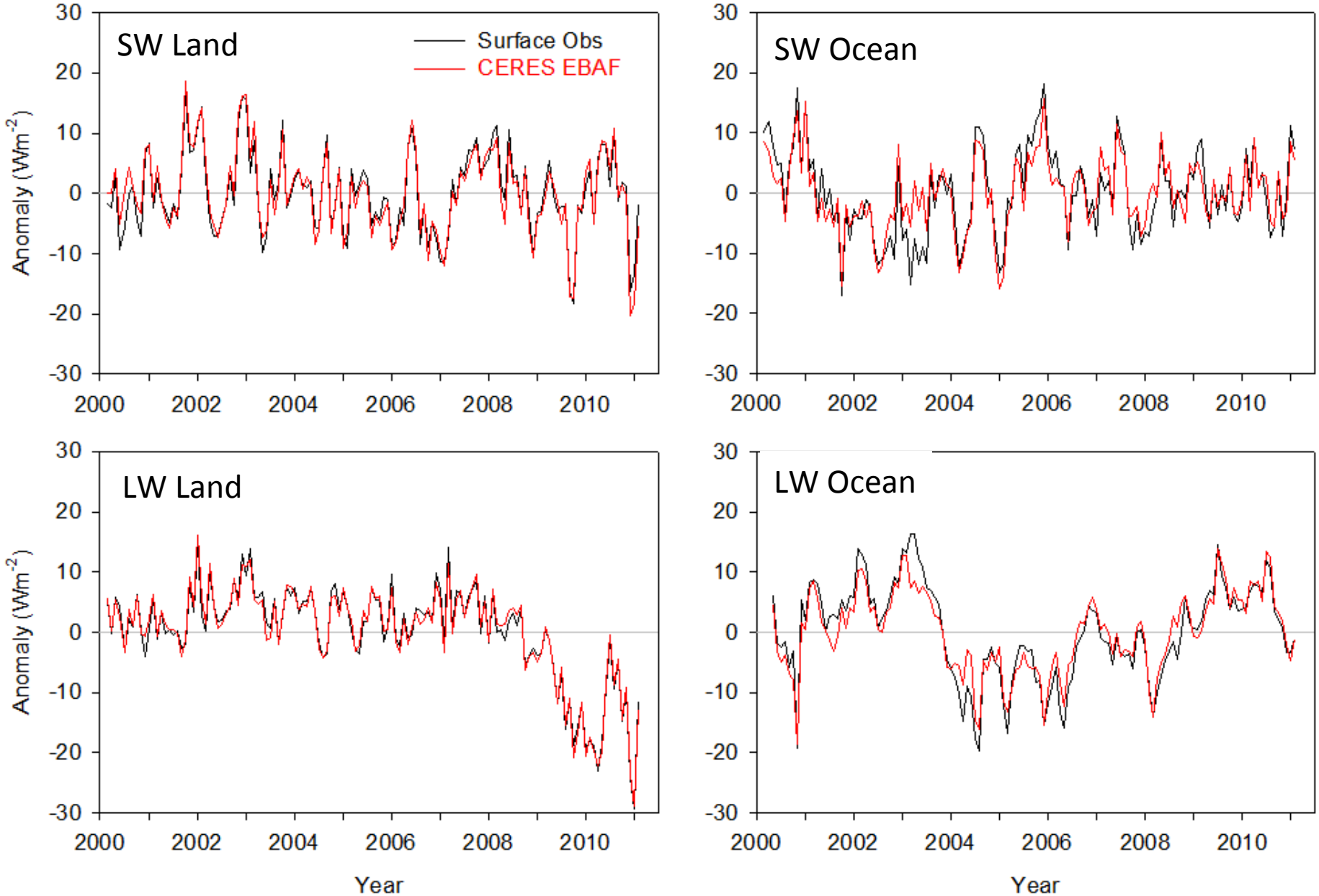

CERES EBAF Downward Surface Flux Comparison with Surface Observations

	SW Land					
	Mean (Wm^{-2})	σ(Mean) (Wm^{-2})	$\sigma(\delta)$ (Wm^{-2})	$\sigma(\delta_C-\delta_O)$ (Wm^{-2})	r	<N>
Surface Obs	180.8	30.1	6.8	1.8	0.97	29.2
CERES EBAF	180.1	29.2	7.0			
	LW Land					
	Mean (Wm^{-2})	σ(Mean) (Wm^{-2})	$\sigma(\delta)$ (Wm^{-2})	$\sigma(\delta_C-\delta_O)$ (Wm^{-2})	r	<N>
Surface Obs	315.1	25.6	8.0	1.1	0.99	29.5
CERES EBAF	315.8	27.0	8.0			
	SW Ocean					
	Mean (Wm^{-2})	σ(Mean) (Wm^{-2})	$\sigma(\delta)$ (Wm^{-2})	$\sigma(\delta_C-\delta_O)$ (Wm^{-2})	r	<N>
Surface Obs	236.0	11.8	7.1	3.1	0.9	17.5
CERES EBAF	240.0	11.3	6.1			
	LW Ocean					
	Mean (Wm^{-2})	σ(Mean) (Wm^{-2})	$\sigma(\delta)$ (Wm^{-2})	$\sigma(\delta_C-\delta_O)$ (Wm^{-2})	r	<N>
Surface Obs	400.1	8.1	7.8	2.7	0.95	5.4
CERES EBAF	398.7	7.0	6.7			

- CERES EBAF surface fluxes are well within uncertainty of surface observations (~ 5 Wm^{-2})

Average (March 2000 – February 2010) Ra, LP, S and H from Satellite Obs & Reanalysis

	SH	Asc	NH	30°S-30°N	Global
Ra(CER)	-115.2	-93.5	-109.5	-106.3	-108.6
Ra(ERAI)	-119.7	-100.7	-107.4	-110.6	-109.2
Ra(Merra)	-118.5	-96.6	-107.4	-108.9	-105.9
LP(GPCP)	59.3	131.6	51.3	88.4	77.6
LP(ERAI)	61.1	159.0	54.4	104.2	82.9
LP(Merra)	54.8	156.1	54.6	101.2	81.0
S(ERAI)	23.1	16.4	26.4	20.6	17.5
S(Merra)	27.4	14.0	26.3	20.3	18.1
H*(CGE)	**-32.9**	**54.5**	**-31.8**	**2.7**	**-13.5**
H*(ERAI)	-35.5	74.7	-26.6	14.2	-8.7
H*(Merra)	-36.3	73.6	-26.6	12.6	-6.8
H(ERAI)	-23.9	77.8	-6.1	23.3	1.4
H(Merra)	-29.3	78.6	0.9	25.3	-0.5

Interannual Anomalies in H: From Diabatic Heating vs Direct Calculations

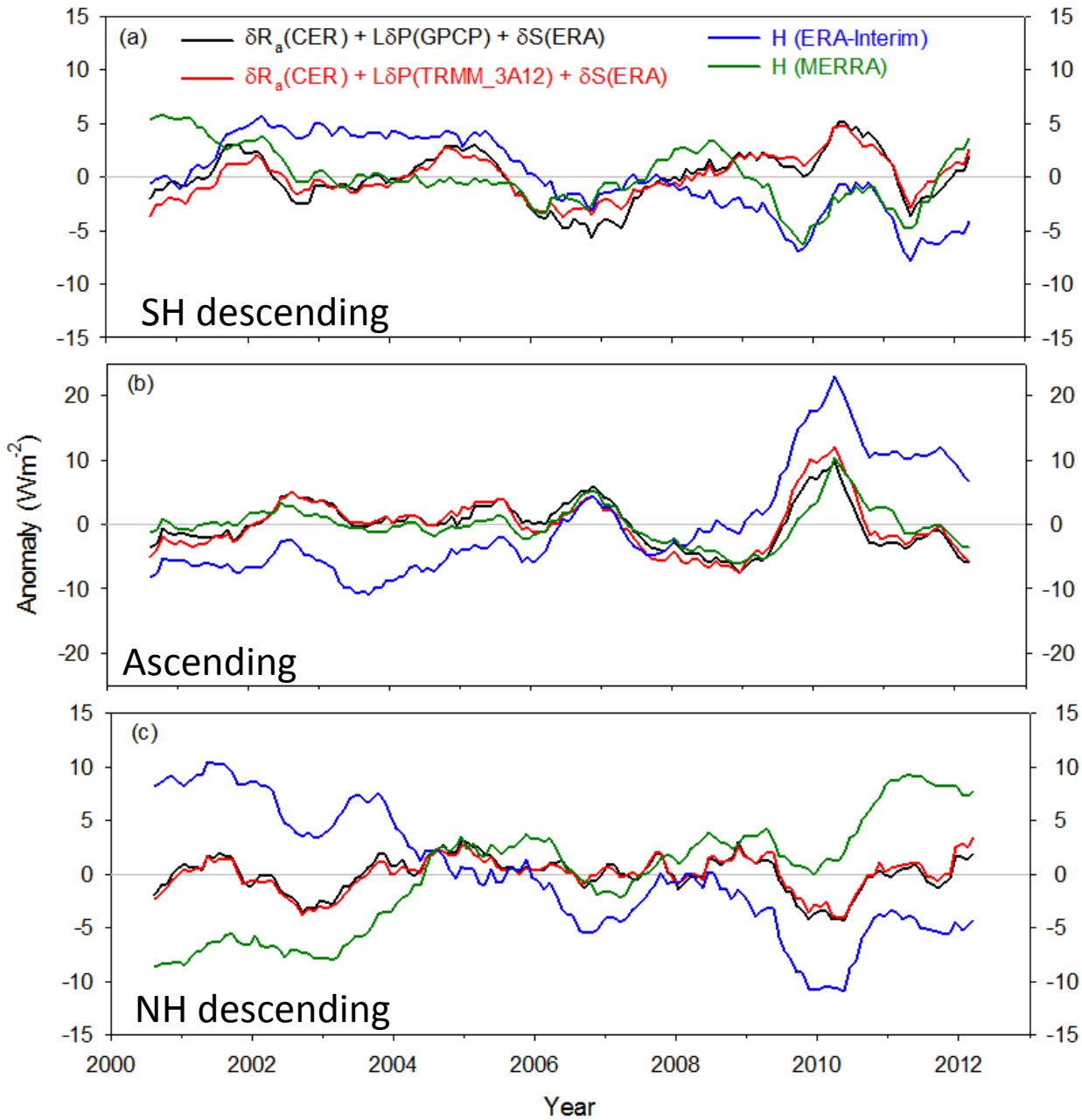

Relationship Between H and Mid-Tropospheric Vertical Velocity

- In the zonal mean, the vertical advective component dominates (Muller and O'Gorman, 2011), so that changes in the divergence of energy transport depend upon changes in mean vertical velocity, mean dry static stability, and their covariance:

$$\delta\left[\int\left(\omega\frac{\partial s}{\partial p}\right)\frac{dp}{g}\right]=\int\left(\delta[\omega]\frac{\partial s}{\partial p}\right)\frac{dp}{g}+\int\left(\omega\,\delta\left[\frac{\partial s}{\partial p}\right]\right)\frac{dp}{g}+\int\left(\delta[\omega]\delta\left[\frac{\partial s}{\partial p}\right]\right)\frac{dp}{g}$$

"Dynamic Component"

"Thermodynamic Component"

Interannual Anomalies in H and ω

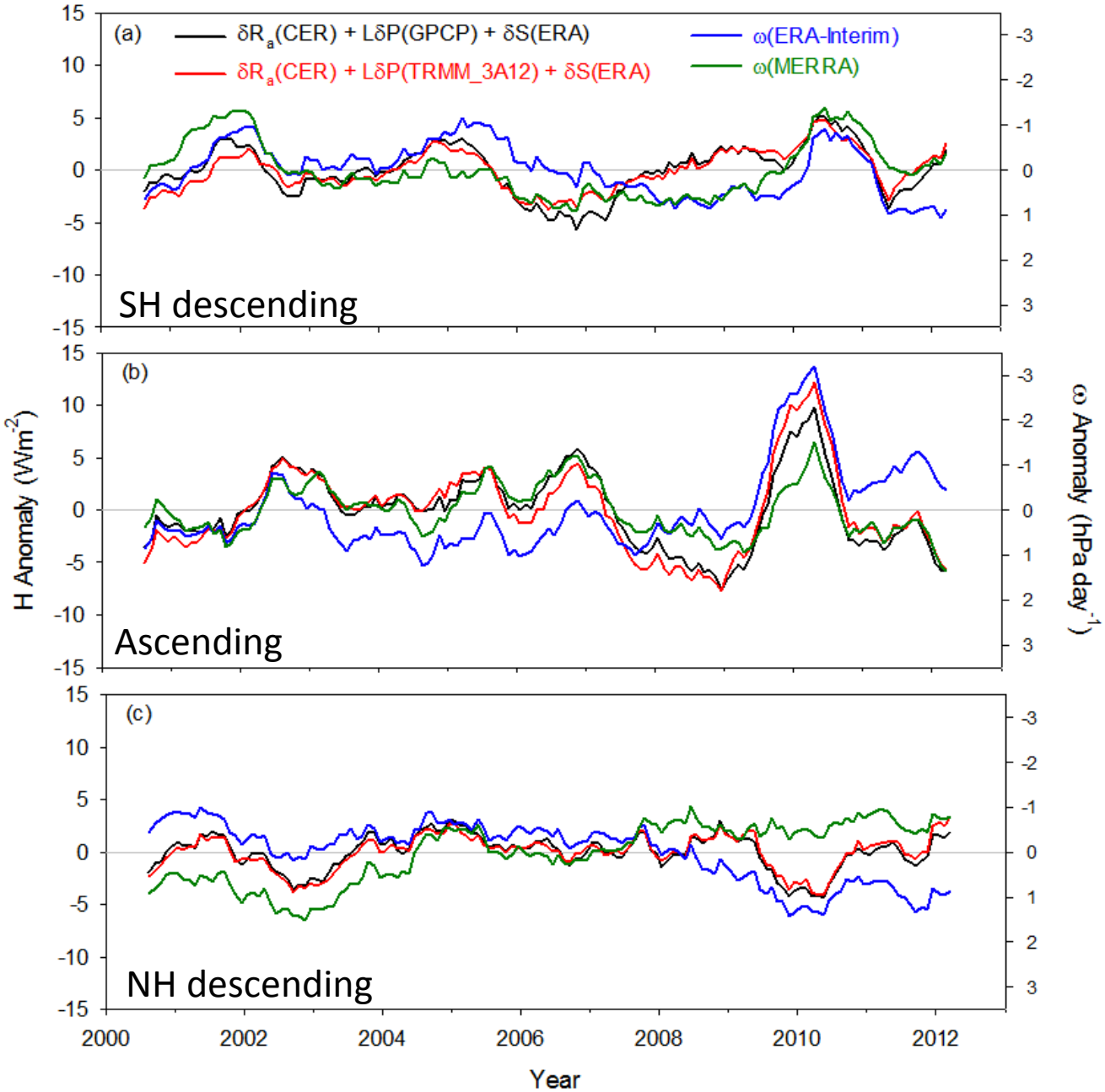

Slope of Anomalies in R_a, LP and S against Anomalies in ω

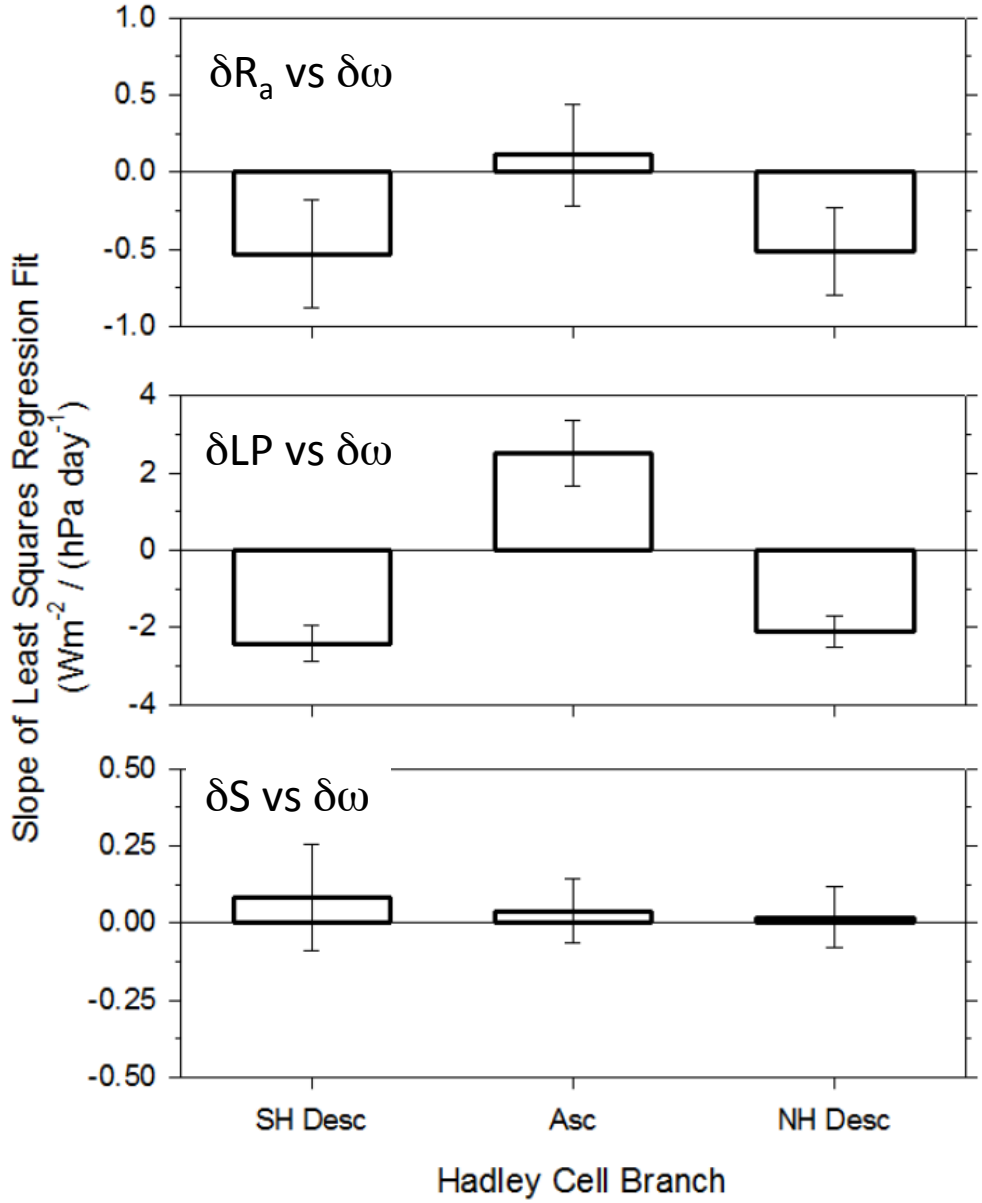

- Sensitivity of LP to ω* is 4-5 times greater than between Ra and ω* in the descending branches, but 20 times greater in the ascending branch.
- Global LP constrained by radiative cooling.
- 20% of the global LP variability is explained by LP variations in the ascending branch.
- 20-25% of the global variability in Ra is explained by Ra variations in the descending branches.

=>Stronger HC thus contributes to enhanced global radiative cooling and latent heating at interannual timescales.

- For convenience, ω is defined as positive up in ascending branch and positive down in descending branches.

Regression Slope of Anomalies in Radiative Flux vs Anomalies in Circulation Strength (ω^*)

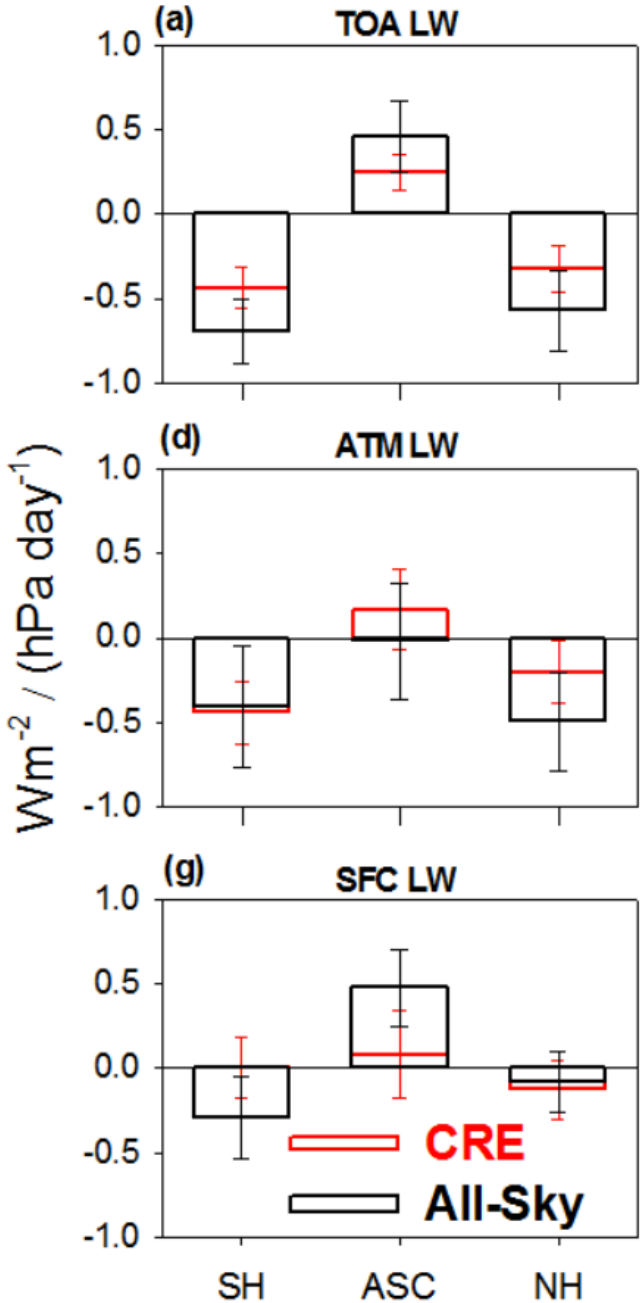

- Increase ascent in ascending branch
  - ⇒ Reduced emission to space
  - ⇒ TOA radiative warming
- Increase subsidence in descending branches
  - ⇒ Increased emission to space
  - ⇒ TOA radiative cooling
- Large contribution by cloud radiative effects

- Ascending branch: Clear-sky LW radiative cooling balanced by radiative warming by clouds

- Lack of CRE sensitivity to ω^* at surface
  - ⇒ Is co-variation associated with high clouds?

Slope of monthly anomalies in cloud frequency of occurrence against monthly anomalies in ω*

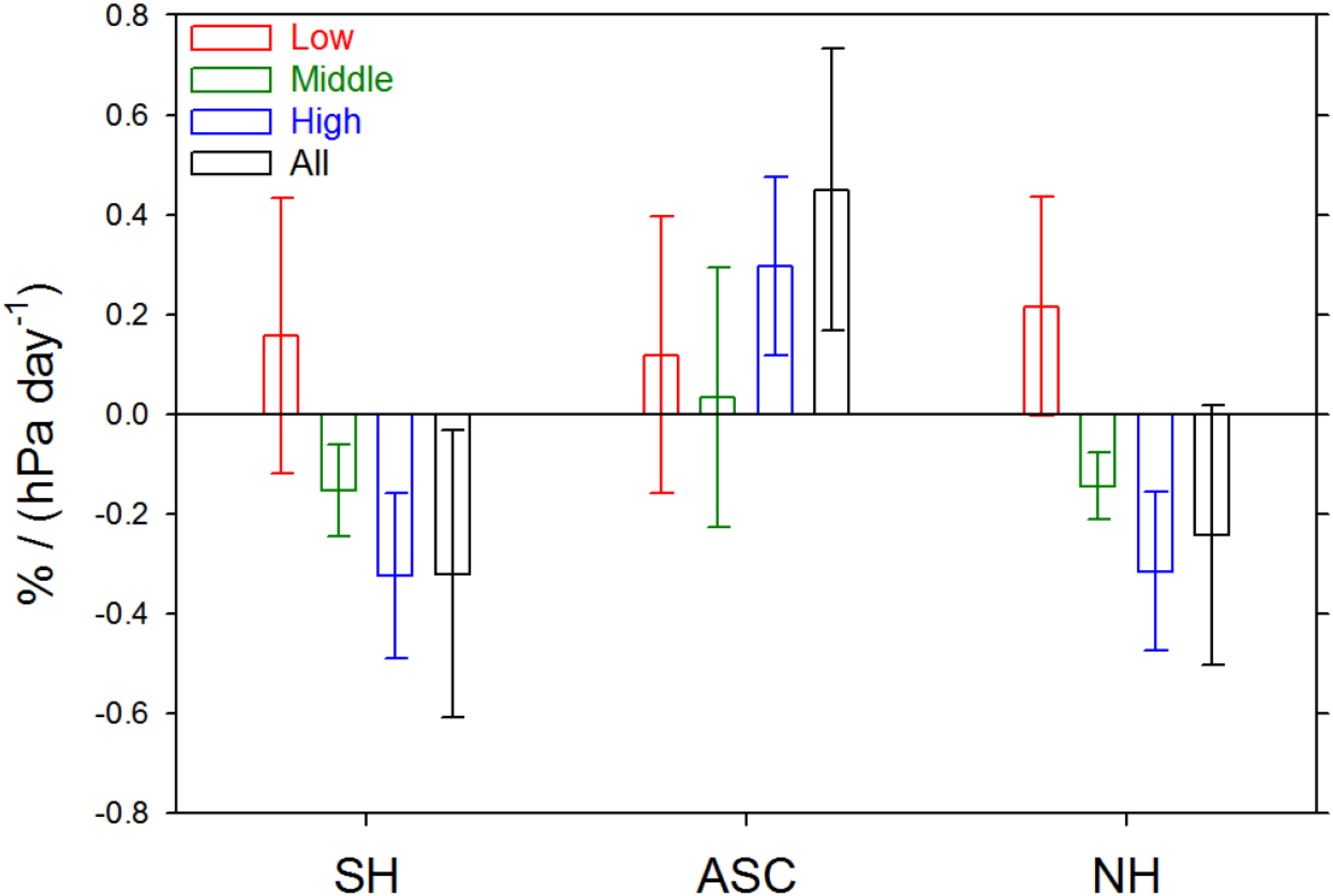

Regression Slope of Anomalies in Radiative Flux vs Anomalies in Circulation Strength (ω^*)

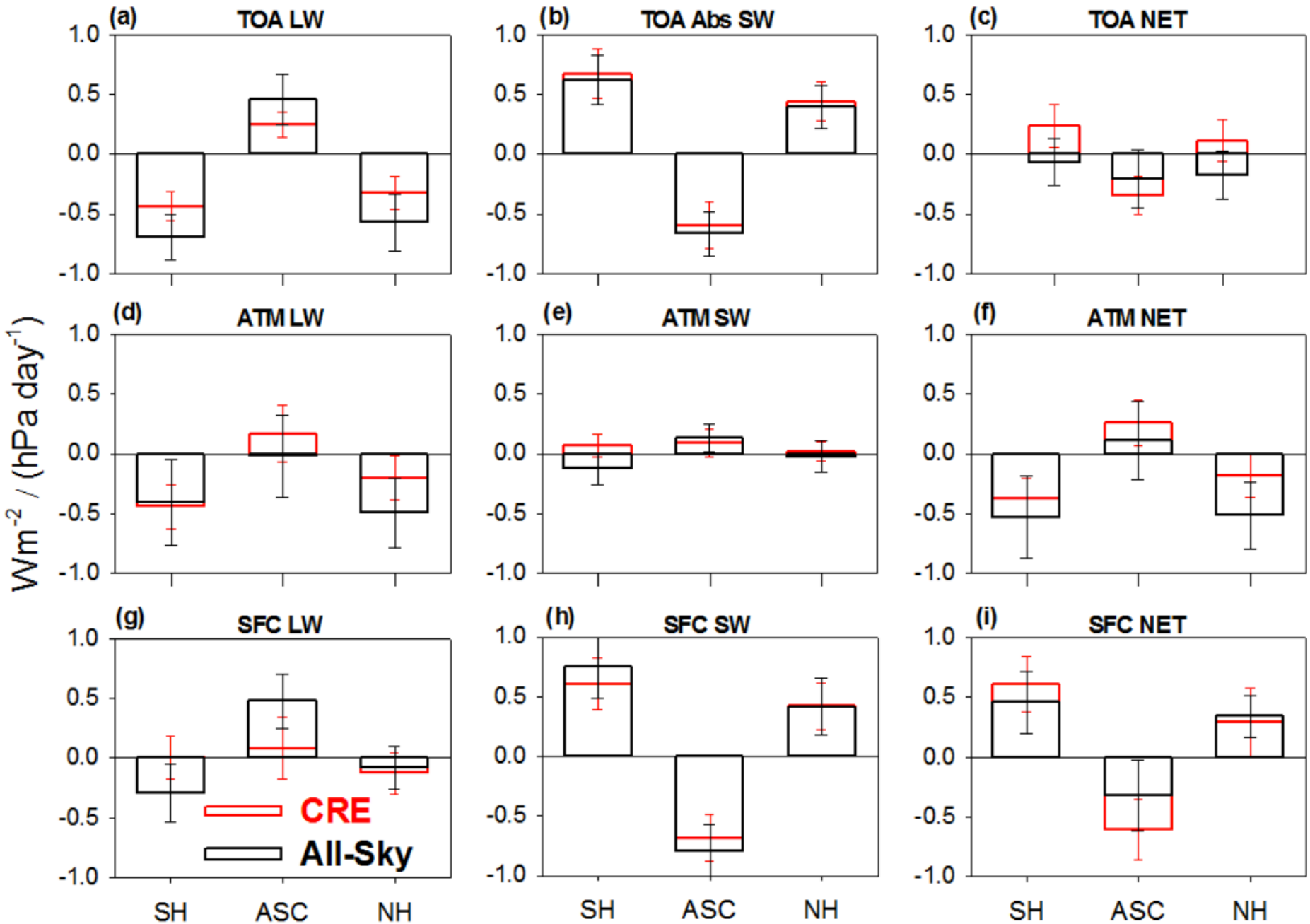

Do Cloud Radiative Effects Increase or Decrease HC Strength?

- As HC circulation strength increases (i.e., ω^* increases), clouds enhance atmospheric radiative cooling in the descending branches but oppose it in the ascending branch.

- This enhances the latitudinal gradient in diabatic heating, potentially leading to an increase in HC strength.

- However, the cloud response also influences convective latent heating in the tropics by altering the dry and moist static stability of the atmosphere.

- Owing to the close coupling between CREs, moist convection and circulation strength, it is exceedingly difficult to draw conclusions about the magnitude and even the sign of the feedback between clouds and HC strength from satellite observations alone.

Impact of the atmospheric cloud radiative forcing on GCM-simulated tropical circulation

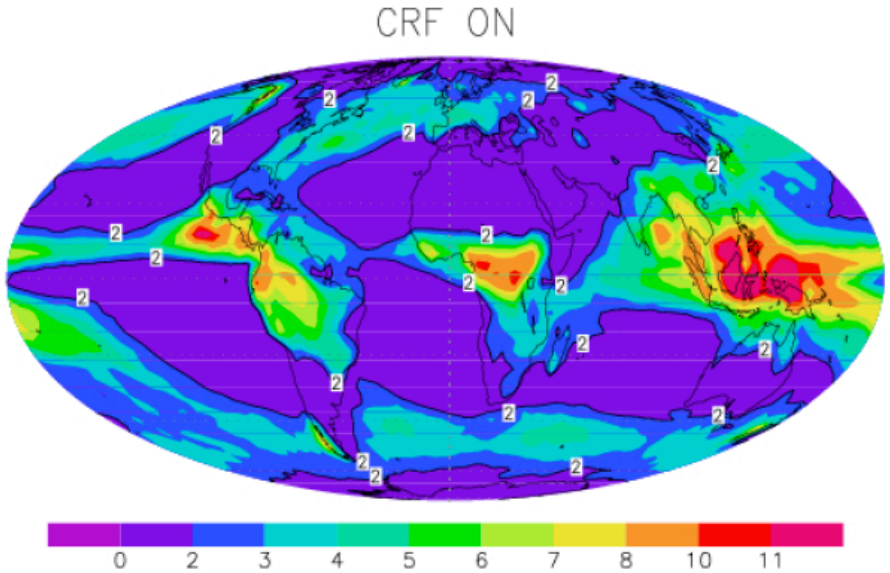

Precipitation (mm/d)

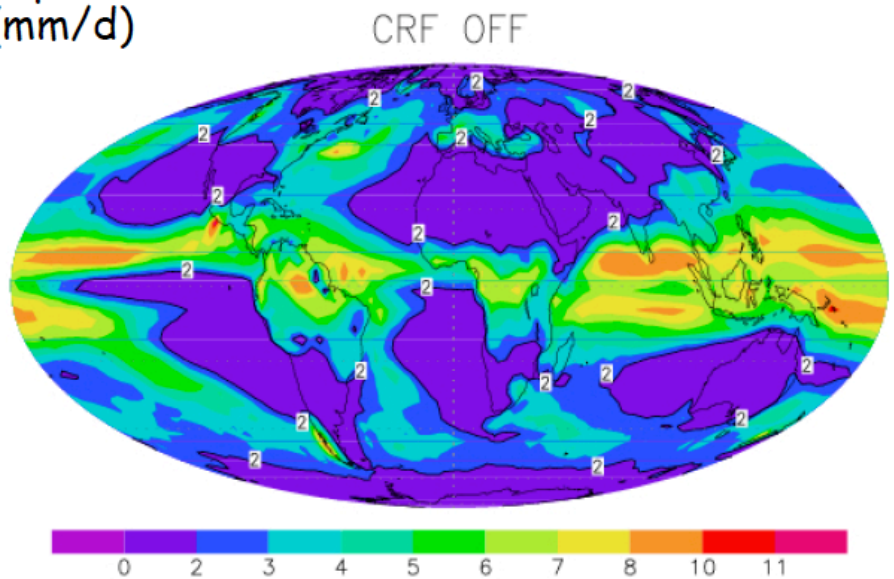

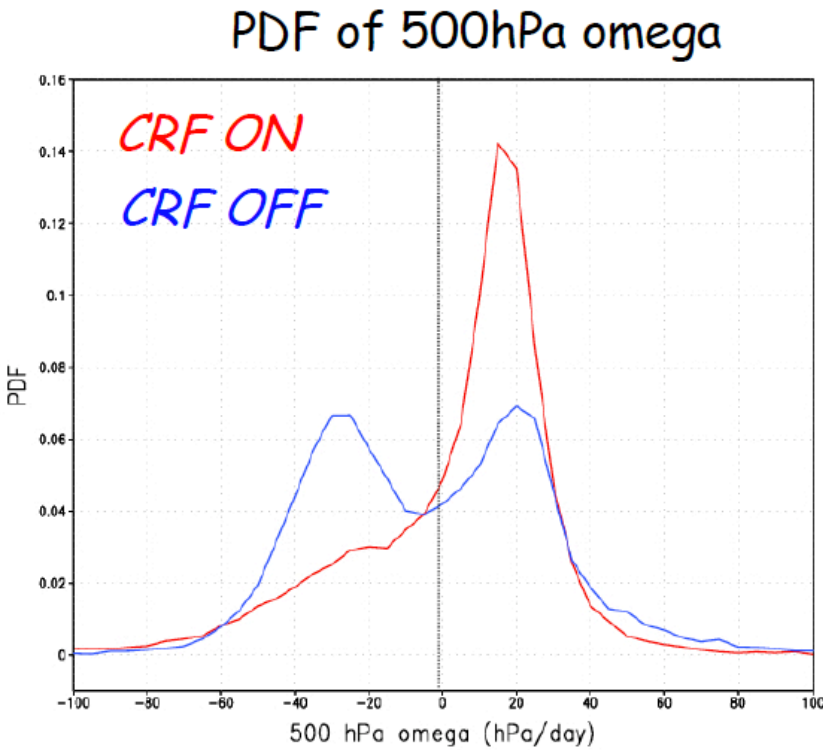

Cloud-radiative effects strengthen the Hadley-Walker circulation and make the ITCZ more narrow

Bony, 2007

Summary

- An energetic perspective is used to show the potential of satellite observations for for tracking changes in large-scale circulation.
- Sorting the data in spatial domains that follow the large-scale circulation is a natural framework for studying co-variability between cloud/radiation/atmospheric state and atmospheric circulation.
- The latitudinal distance between southern and northern hemisphere LW CRE subtropical minima can be used to monitor changes in the latitudinal extent of the deep tropics.
- The close relationship between divergence of DSE and vertical velocity in the 3 branches of the HC offers an alternative approach to for tracking changes in the strength of the HC (i.e., through satellite observed diabatic heating).

- We find a -14 Wm^{-2} imbalance in the global mean atmospheric energy budget, suggesting that either global radiative cooling is overestimated and/or latent and/or sensible heating are underestimated.

-> See no evidence of a large bias in satellite-based TOA and surface radiation budgets.

-> Differences amongst precipitation datasets largest in ascending branch, where precipitation is strongest.

- As HC circulation strength increases, clouds enhance radiative cooling in the descending branches but oppose it in the ascending branch.
  - Cloud radiative effects enhance the latitudinal gradient in diabatic heating, potentially leading to an increase in HC strength.
  - However, clouds can also have a strong indirect influence on diabatic heating and circulation by altering the local distribution of atmospheric heating, giving rise to further changes in latent heating.

END